COSMO-based/Aspen Plus process simulation of the aromatic extraction from pyrolysis gasoline using the {[4empy][NTf_2] + [emim][DCA]} ionic liquid mixture

Marcos Larriba,[a,*] Juan de Riva,[a] Pablo Navarro,[b] Daniel Moreno,[a] Noemí Delgado-Mellado,[c] Julián García,[c] Victor R. Ferro,[a] Francisco Rodríguez,[c] José Palomar[a]

[a]*Sección de Ingeniería Química, Universidad Autónoma de Madrid, 28049 Madrid, Spain*

[b]*CICECO – Aveiro Institute of Materials, Department of Chemistry, University of Aveiro, Aveiro, Portugal*

[c]*Departamento de Ingeniería Química, Universidad Complutense de Madrid, 28040 Madrid, Spain*

Abstract

The ionic liquids (ILs) have been widely studied as potential replacements of conventional solvents in the extraction of aromatic hydrocarbons from alkanes. However, most of the literature is focused in obtaining liquid-liquid equilibria experimental data without studying the complete extraction and IL regeneration process. In this paper, a computer-aided methodology combining COSMO-based molecular simulations and Aspen Plus process simulations has been used to study the extraction process of aromatic hydrocarbons from pyrolysis gasoline employing a binary mixture of 1-ethyl-4-methylpyridinium bis(trifluoromethylsulfonyl)imide ([4empy][NTf_2]) and the 1-ethyl-3-methylimidazolium dicyanamide ([emim][DCA]) ILs as solvent. An extensive comparison (more than 600 points) between experimental data and the predictions obtained by the COSMO-based thermodynamic model of liquid-liquid and vapor-liquid equilibria and ILs physical properties was made for validation purposes. Process simulations were performed in three system configurations: with one, two, or three flash distillations in the IL recovery section. The potential advantage of using binary IL-IL mixture as extracting solvent was studied in the whole range of composition. The configuration with three flash distillations and the binary IL-IL mixture with a 75 % of [4empy][NTf_2] were selected as the optimal conditions to increase aromatic recovery and purity, improving the separation performance respect to the neat ILs.

Keywords: Aromatic-aliphatic separation; Ionic liquids; Aspen Plus; COSMO-RS; Process Simulation.

[*]Corresponding author. E–mail address: marcos.larriba@uam.es (Marcos Larriba).

1. Introduction

Pyrolysis gasoline is the main source of benzene, toluene, and *p*-xylene (BTX) because of its high aromatic content (50-70 wt. %) [1]. The separation of BTX from the alkanes is normally performed by liquid-liquid extraction processes employing organic solvents [2]. The Shell-UOP Sulfolane Process is the most commonly used process for the dearomatization of petroleum streams. However, this process has several drawbacks caused by the volatility of the sulfolane and the partial solubility of the solvent in the alkanes. The use of ILs in the dearomatization of pyrolysis gasoline could reduce energy consumption and operating costs of this unit due to the nonvolatile nature of ILs and the negligible solubility of the majority of ILs in alkanes [3].

Because of this, a wide number of ILs have been tested in the separation of aromatic hydrocarbons from alkanes. Nevertheless, the majority of papers in this field have been focused on the extraction of one aromatic hydrocarbon from one alkane without studying the simultaneous extraction of several aromatics or the subsequent separation of the extracted hydrocarbon from the IL [4-6]. In our recent publications, we have experimentally studied the extraction of aromatic hydrocarbons using ILs and the vapor-liquid separation of the extracted hydrocarbons from the IL-based solvents [7-9].

We also proposed the use of binary IL-IL mixtures to obtain a solvent with intermediate physical and extractive properties between the pure ILs forming the mixture [10]. In these works, we obtained a IL-based solvent with extractive properties similar to sulfolane, mixing an IL with a high aromatic distribution ratio, [4empy][NTf_2], with an IL with high aromatic/aliphatic selectivities, [emim][DCA] [10,11]. This binary IL-IL mixture was selected to be employed in this work in the simulation of the complete extraction process of aromatics from pyrolysis gasoline. The binary IL-IL mixtures have been also applied in other separation processes such as CO_2 capture or SO_2 absorption [12,13]. In addition, the behavior of IL mixtures have been deeply studied analyzing the experimental data available in literature [14-16], while the Conductor-like Screening Model for Real Solvents (COSMO-RS) methodology was successfully employed to predict the mixing behavior of IL mixtures [17].

COSMO-based calculations were also previously used in the prediction of the performance of ILs in separation processes [18-23]. In this work, we have evaluated the applicability of COSMO-based thermodynamic models in the prediction of liquid-liquid and vapor-liquid equilibria for systems composed of BTX, *n*-alkanes, and the ILs [4empy][NTf_2] and [emim][DCA]. In addition, the physical property predictions of the {[4empy][NTf_2] + [emim][DCA]} mixtures were also validated.

In our last publications, we used a multiscale computational methodology to simulate and optimize IL-based separation processes [24-30]. The first step in this strategy is to validate the predictions obtained by the COSMO-based methodology, because the COSMOSAC property model will be employed in the Aspen Plus process simulator to calculate the activity coefficients. This multiscale methodology has been successfully applied to simulate the application of ILs in the IL regeneration by distillation [24], the separation of aromatic hydrocarbons from aliphatics [25,29], the absorption refrigeration cycles [27], the absorption of toluene [28], and the CO_2 capture by physical absorption [30,31].

The simulations in this work had a double aim: to study the role of the composition in the IL mixture and to select the most adequate configuration in the extraction process of aromatic hydrocarbons from pyrolysis gasoline using IL-based solvents. Several configurations have been proposed to perform the extraction of BTX from petroleum streams using ILs. In all these proposals, the extraction is performed in a countercurrent liquid-liquid extraction column but the recovery section of the extracted hydrocarbons from the IL-based solvent are significantly different. Due to the nonvolatile character of the IL, the separation of the extracted hydrocarbons could be easily performed by flash distillations [32].

The simplest configuration is depicted in Fig. 1 and is formed by an extraction column and a flash distillation [25]. Recently, two new configurations have been proposed being the recovery section formed by two and three flash distillations [33]. The flow diagram of these configurations are showed in Fig. 2 and Fig. 3. The objective of employing more than one flash distillation is to take advantage of the performance of ILs as entrainers in the vapor-liquid separation of aromatic and aliphatic hydrocarbons. In the first or two first flash distillations, a selective evaporation of the aliphatic hydrocarbons would be made and the last flash would be employed to remove the remaining aromatic hydrocarbons from the IL-based solvent [33]. In this work, the three described configuration were simulated in Aspen Plus using the {[4empy][NTf_2] + [emim][DCA]} IL mixture. First, the role of the IL mixture composition was evaluated considering the separation performance (recovery and purity of aromatic product) and the energy needs to select the most adequate composition in the mixture. The solvent to feed ratio (S/F) was also studied in the liquid-liquid extraction processes to optimize the solvent consumption. For each configuration, the effect of the S/F on the separation performance and energy needs was also studied.

2. Computational Details

2.1. DFT and COSMO-RS calculations

The molecular geometry of the ILs (Tables S1 and S2 in Supplementary Material) was optimized by using the DFT method B88-P86 (bp) and TZVP basis set with RI approximation with TURBOMOLE software. A molecular model of ion-pair was used to describe the IL, where cation and anion structures were treated as a whole. Different ion-pair conformers were optimized, selecting that with the lowest electronic energy for later calculations. Subsequently, the .cosmo file (used as input in COSMOthermX software) were generated by applying the COSMO solvation model [34] at the same quantum-chemical computational level. Then, COSMO-RS calculations were performed in the COSMOthermX program package (version C30_1201, BP_TZVP_C30_1201 default parametrization) [35,36] to obtain the required information to defile IL pseudo-component: molecular volume, σ-profile, density, molecular weight and normal boiling temperature. This methodology has been deeply described in our previous publications [24-30].

2.2. Component definition

To perform the process simulation, the [4empy][NTf_2] and [emim][DCA] ILs were defined as pseudo-component in the Aspen Plus V 8.8 process simulator. The following ILs' properties were added in the simulator to define the pseudo-component: density, molecular weight, normal boiling temperature and viscosity. Density and normal boiling temperature were calculated using COSMO-RS method with COSMOthermX software as previously described. The experimental viscosities of the ILs were obtained from literature and fitted to an Arrhenius type equation to the corresponding A and B parameters following the procedure published previously [38], to be included in IL pseudo-component definition. In addition, the sigma-profiles and molecular volumes of the ILs obtained from COSMOthermX results were introduced in Aspen Plus simulator to completely specify the COSMO-SAC property model. All the information used to define the [4empy][NTf_2] and [emim][DCA] ILs as pseudo-component in the Aspen Plus is available in Tables S1 and S2 of Supplementary Material. More information on this computational approach was reported in the documentation of free ILUAM database, recently published with information available for 100 common ILs [39].

Subsequently, viscosities, heat capacities and surface tensions of ILs and their mixtures used in process simulations of this work were estimated using the default methods implemented in the Aspen Properties system for pseudo-components. In the case of density of binary IL mixtures, the VLMX26 method was used to ensure the consistency with the density of the pure ILs [40]. Hydrocarbons forming the pyrolysis gasoline: benzene, toluene, *p*-

xylene, *n*-hexane, *n*-heptane, and *n*-octane were selected as conventional components from the Aspen Plus database.

2.3 Conceptual design for the extraction of aromatic hydrocarbons using ionic liquid-based solvents

The most usual composition of the pyrolysis gasoline was obtained from Franck and Stadelhofer (1988) and reported in Table 1 [1]. The flow of pyrolysis gasoline introduced to the process was fixed to 100 kg/s in all simulations. To determine the optimal composition in the IL mixture, simulations employing the {[4empy][NTf_2] + [emim][DCA]} mixture as solvent with a 0 %, 25 %, 50 %, 75 %, and 100 % of [4empy][NTf_2] were carried out. As explained in the introduction, three configurations were also tested to select the most appropriate to be employed in the dearomatization of the pyrolysis gasoline using the binary IL-IL mixture.

2.3.1. Configuration 1

The flow diagram of the Configuration 1 is depicted in Fig. 1. This configuration is formed by a countercurrent liquid-liquid extraction column (T-100) whereas a single flash distillation (V-100) forms the recovery section. The extraction column operates at 40 ºC and 1 atm, since these conditions are the most employed in the extraction of aromatic hydrocarbons using ILs [5,41,42]. The temperature of the flash distillation was fixed to 120 ºC and a high vacuum was used (10 mbar) to ensure the volatilization of the extracted hydrocarbons from the IL mixture. The selected temperature was lower than the experimentally determined maximum operation temperature (139 ºC) that allows the employment of the {[4empy][NTf_2] + [emim][DCA]} IL mixture for 1 year without thermal decomposition [43].

In this configuration, the IL-based solvent (S-01) and the pyrolysis gasoline (S-02) are introduced to the extraction column obtaining a raffinate stream (S-03) and an extract stream (S-04). The extract stream is heated to 120 ºC in heat exchangers E-101 and E-102 before being introduced into the flash distillation (V-100). In the recovery section, a liquid stream composed mainly by the IL mixture (S-07) is obtained. This stream is conditioned in the heat exchangers E-100 and E-101 and in the pump P-100 to be recycled to the extractor. In the flash distillation (V-100) a vapor stream formed by hydrocarbons (S-08) is also obtained and conditioned to the temperature and pressure of the extractor in a compressor (C-100) and a heat exchanger (E-103). A 10 % of this stream was recycled to the extraction column (S-12) whereas the remaining 90 % was obtained as aromatic product (S-11). This percentage was selected to ensure high values of aromatic recovery. As can be seen in Fig. 1., the

Configuration 1 has two recycle loops from the recovery section to the extractor, one formed by the regenerated IL mixture and the other composed of hydrocarbons.

2.3.2. Configuration 2

The flow diagram for the second configuration tested in this work is shown in Fig. 2. As seen, the extraction section is analogue to that described for the Configuration 1 but the recovery section includes two flash distillations. The first flash distillation (V-100) operates at 60 ºC and 300 mbar to selectively recover the extracted aliphatic hydrocarbons from the IL-based solvent. These conditions were selected considering the experimental results obtained in the selective recovery of *n*-heptane from BTX and the {[4empy][NTf_2] + [emim][DCA]} IL mixture [44]. In V-100, a vapor stream (S-07) is obtained and conditioned to be recycled to the extractor, whereas the liquid stream formed mainly by aromatic hydrocarbons and the IL mixture (S-06) is send to the second flash distillation. Temperature and pressure of this second flash distillation (V-101) were coincident with those described for the flash in the Configuration 1 (120ºC and 10 mbar) to promote the vaporization of the hydrocarbons from the IL mixture. The vapor stream obtained in V-101 is compressed to 1 atm and cooled to 40 ºC to obtain the aromatic product stream. The IL-mixture stream from the V-101 (S-11) was also conditioned before recycling to the extractor.

2.3.3. Configuration 3

In Fig.3, the flow diagram for the Configuration 3 is depicted. The extraction column in this configuration operates under the same conditions previously described. In this case, the recovery section is formed by three flash distillations. The two first are destined to selectively evaporate the extracted aliphatic hydrocarbons and in the third flash all the remaining hydrocarbons are evaporated from the IL mixture. The operating conditions of the first, second, and third flash distillations were 60 ºC and 300 mbar, 60 ºC and 200 mbar, and 120 ºC and 10 mbar, respectively. The vapor streams (S-07 and S-11) obtained in the two first flash distillations (V-100 and V-101) are recycled to the extraction column (T-100) to increase the purity and recovery of the aliphatic hydrocarbons obtained in the raffinate stream. The liquid stream from the third flash (V-102) formed by the IL mixture was also recycled to T-100 and the vapor stream (S-18) is the aromatic product. In Configuration 3, three recycle loops were used and this fact complicates the convergence of the simulations.

2.4. Separation units modeling

To simulate the countercurrent liquid-liquid extraction column the Aspen Plus EXTRACT rigorous model was employed. The simulator used the COSMOSAC property model to

calculate the activity coefficient of the compounds. In all the simulations, the adiabatic extraction column was configured to have 20 equilibrium stages and to operate at 40 ºC and 1 atm. The IL-based solvent was fed to the first stage while the pyrolysis gasoline stream was introduced in the stage 20. The recycled streams were introduced in the stages 18 and 19 of the extraction column due to their significant contents in aromatic hydrocarbons. The IL mixture was defined as the heavy key component in the extractor, whereas the *n*-hexane was the light key component. On the other hand, the flash distillations were simulated using the FLASH2 model of Aspen Plus. The operating conditions in the flash distillation were previously described for each configuration. Finally, the 1-way heat exchangers were simulated using the HEATER model and HEATX model was employed to simulate the 2-way heat exchangers. From the duty calculated for the HEATER models, cooling and heating needs for each configuration were calculated.

3. Results and discussion

3.1. Validation of predictions of equilibria using COSMO-based methodology

The validation of the predictions is a needed step before performing a process simulation using a predictive model as COSMOSAC in Aspen Plus. For this reason, we have compared the liquid-liquid equilibria and vapor-liquid equilibria experimental data of systems composed of the hydrocarbons forming the pyrolysis gasoline and the [4empy][NTf_2] and [emim][DCA] ILs. In addition, a comparative analysis between the experimental and predicted densities, dynamic viscosities, surface tensions, and specific heats of the {[4empy][NTf_2] + [emim][DCA]} binary IL-IL mixture has been performed. To evaluate the reliability of the predictions, the mean deviation of each estimated property was calculated with respect to experimental values available in literature and correlation coefficients (R^2) were calculated in the fitting of experimental against predicted values.

3.1.1. Validation of the liquid-liquid equilibria and vapor-liquid equilibria of hydrocarbons + [4empy][NTf_2] and [emim][DCA] pure ionic liquids

To adequately simulate the liquid-liquid extractor in Aspen Plus, the liquid-liquid equilibria between the hydrocarbons and the ILs have to be successfully predicted by the COSMO-based/Aspen Plus approach. In Fig. 4, the literature liquid-liquid equilibria for the {*n*-heptane + toluene + [emim][DCA]} and {*n*-heptane + toluene + [4empy][NTf_2]} ternary systems at 313.2 K [37,45] are plotted together with the predictions using COSMO-based

calculations. As observed, the COSMO-based/Aspen Plus methodology predicted the negligible solubility of both ILs in the raffinate phase. Moreover, in the case of the [emim][DCA], the slopes of the predicted tie lines were almost coincident with those of the experimental tie lines and the low solubility of *n*-heptane in this IL was also adequately predicted. COSMO-based/Aspen Plus approach also reasonably predicted the liquid-liquid equilibria in the presence of [4empy][NTf_2], but with higher deviations than that for the [emim][DCA]. Correlation coefficients (R^2) and predicted compositions mean deviations (Δx) in the fitting of experimental and predicted liquid-liquid equilibria by the COSMO-based methodology of the ternary systems involving pure ILs are listed in Table 2, presenting values of R^2 higher than 0.98.

In the proposed processes, the recovery section of the extracted hydrocarbons from the IL mixture is formed by flash distillations. Because of this, the vapor-liquid equilibria between the hydrocarbons and the [4empy][NTf_2] and [emim][DCA] has been also validated. In Fig. 5, the literature [9] and predicted vapor-liquid equilibria for the binary systems {*n*-heptane + [emim][DCA]} and {toluene + [emim][DCA]} at 323.2, 343.2, and 363.2 K are depicted as pressure (P) - composition in the liquid phase (x_i) diagrams. In Table 3, correlation coefficients (R^2) and mean deviation of predicted pressures (ΔP) with respect to experimental data are listed. Analyzing the values of R^2 and ΔP, we can conclude that the predictions by COSMO-Aspen Plus approach were very similar to the literature values experimentally obtained.

The literature and predicted vapor-liquid equilibria for the {*n*-heptane + [4empy][NTf_2]} and {toluene + [4empy][NTf_2]} are plotted in Fig. 6 [46]. As in the case of the liquid-liquid equilibria, the predictions for the systems formed by the [4empy][NTf_2] agreed reasonably with experimental data, but again exhibited slightly higher deviations, as can be compared from the values of R^2 and ΔP in Table 3. The COSMO-based model estimated a solubility of *n*-heptane in the [4empy][NTf_2] higher than the experimental value, as can be inferred for the lower slope in the *P*-*x* diagram, since the maximum solubility of the hydrocarbon in the IL is the point where the *P*-*x* diagram becomes horizontal. A similar behavior is observed in the {toluene + [4empy][NTf_2]} particularly at the highest temperature, 363.2 K. Despite these small deviations, the predictability of the *a priori* COSMO-Aspen Plus approach is considered adequate to perform the conceptual design of the studied separation process involving liquid-liquid extraction and vapor-liquid solvent recovery stages.

3.1.2. Validation of the liquid-liquid equilibria and vapor-liquid equilibria of hydrocarbons + the {[4empy][NTf$_2$] (0.3) + [emim][DCA] (0.7)} binary IL-IL mixture

Once the validation of the liquid-liquid and vapor-liquid equilibria of the systems formed by the hydrocarbons and the [4empy][NTf$_2$] and [emim][DCA] pure ILs was made, a similar validation has been performed using the {[4empy][NTf$_2$] + [emim][DCA]} binary IL-IL mixture. Fig. 7 shows a comparison of the experimental and predicted liquid-liquid equilibria for the pseudo-ternary systems formed by {*n*-hexane, or *n*-heptane, or *n*-octane}, toluene, and the {[4empy][NTf$_2$] + [emim][DCA]} binary IL-IL mixture with a [4empy][NTf$_2$] mole fraction of 0.3. This composition was selected because a wide number of experimental data of liquid-liquid and vapor liquid-equilibria were obtained for this composition in the IL mixture in previous publications [10,11,44,47].

Correlation coefficients (R^2) and mean deviation of predicted compositions (Δx) between the experimental and predicted liquid-liquid equilibria by the COSMO-based methodology are listed in Table 2. Very similar experimental and predicted tie lines slopes were observed in the ternary diagrams for the extraction of toluene from *n*-heptane or *n*-octane, being the highest deviations observed in the extraction of toluene from *n*-hexane. Therefore, we may conclude that the COSMO-based/Aspen Plus approach has been revealed as a useful method to predict the liquid-liquid equilibria between aromatic and aliphatic hydrocarbons and the {[4empy][NTf$_2$] + [emim][DCA]} binary IL-IL mixture.

The vapor-liquid equilibria between the aromatic and aliphatic hydrocarbons forming the pyrolysis gasoline and the {[4empy][NTf$_2$] + [emim][DCA]} binary IL-IL mixture with a [4empy][NTf$_2$] mole fraction of 0.3 has been predicted using the COSMO-based methodology and compared with the literature values [44,47]. Predicted and experimental vapor-liquid equilibria of the pseudoternary systems formed by *n*-hexane, *n*-heptane, or *n*-octane and the {[4empy][NTf$_2$] (0.3) + [emim][DCA] (0.7)} are depicted in Fig. 8. Predictions of the vapor-liquid equilibria agreed with the conclusions drawn from the liquid-liquid equilibria. The COSMO-based/Aspen Plus method slightly overestimated the solubility of the *n*-hexane in the IL mixture with respect to the literature values, whereas the predictions for *n*-heptane and *n*-octane were very similar to the experimental results. Correlation coefficients (R^2) and mean deviation of predicted pressures (ΔP) using the COSMO-based methodology are summarized in Table 3. In Fig.9, the predictions of the vapor-liquid equilibria for the aromatic hydrocarbons and the IL mixture are also plotted together with the literature values [44]. Experimental and predicted values for the three pseudobinary system were similar, as can be observed in the *P-x* diagram and in the high values of R^2 showed in Table 3.

In sum, current results showed that the COSMO-based predictions performed in Aspen Plus guaranties the accuracy level required in the conceptual design of aromatic separation processes from pyrolysis gasoline stage using binary IL-IL mixtures, involving the simulation of both the liquid-liquid extraction column and the subsequent solvent regeneration and hydrocarbon recovery section.

3.1.3. Validation of the physical properties of the {[4empy][NTf$_2$] + [emim][DCA]} binary IL-IL mixture

To ensure the reliability of the results obtained in the simulations by Aspen Plus, a validation of the predicted physical properties for the IL-based solvent has been also performed, comparing with the literature values of density, viscosity, surface tension and specific heat of the {[4empy][NTf$_2$] + [emim][DCA]} binary IL-IL mixture [10,43]. Fig. 10 shows a comparison of estimated and experimental densities as a function of composition in the IL mixture and at temperatures between 293.2 K and 353.2 K. As can be seen, the estimated densities by the COSMO-Aspen Plus approach were very close to the experimental values, showing the correlation coefficients (R^2) and mean deviation of predicted densities in the Table 4. In this case, slightly higher deviations were observed in the mixtures with a high content in [emim][DCA]. The effects of temperature and composition on the densities of the IL mixture were successfully predicted by the COSMO-based methodology.

An Arrhenius-type equation was employed to fit the experimental dynamic viscosities of the IL mixture from the literature values for the viscosities of the pure [4empy][NTf$_2$] and [emim][DCA] ILs. The reliability of this equation was confirmed in our previous publication [38]. The parameters A and B for the Arrhenius equation were introduced to Aspen Plus simulator and the viscosities of the IL mixture were calculated as a function of temperature and composition. Experimental and calculated dynamic viscosities of the {[4empy][NTf$_2$] + [emim][DCA]} binary IL-IL mixture are also depicted in Fig. 10. As can be observed, the predictions exhibited a high reliability with a mean deviation of 0.44 mPa·s with respect to the literature property values, as listed in Table 4. As in the case of density, viscosity prediction adequately described the influence of composition and temperature in this physical property of the IL mixture.

In the liquid-liquid extraction properties, the surface tension of the solvent is also a key parameter. In addition, to calculate the heat and cooling needs of an industrial process of liquid-liquid extraction, the specific heat of the solvent must be adequately described in the simulations. For these reasons, the literature values of surface tensions and specific heats of the {[4empy][NTf$_2$] + [emim][DCA]} mixture [43] have been compared with the predictions

employing the COSMO-based/Aspen Plus integrated tool in Fig. 11. Predicted and experimental specific heats were almost coincident over the whole range of temperatures and compositions with a mean deviation of 3.72 $kJ \cdot kmol^{-1} \cdot K^{-1}$ and the correlation coefficient showed in Table 4. Hence, the calculations of heat requirements in the simulation of the liquid-liquid extraction process will have a high reliability. Finally, the calculated values of the surface tension for the IL-IL mixture were also validated obtaining a deviation of the predictions with respect to the experimental values of 0.91 $mN \cdot m^{-1}$.

3.2. Analysis of the role of {[4empy][NTf$_2$] + [emim][DCA]} mixture composition on separation performance

Once the predictions were validated, the COSMO-based/Aspen Plus integrated tool was employed to study the effect of the IL mixture composition on the extracting solvent properties and to select the most adequate configuration to perform the extraction of benzene, toluene, and *p*-xylene from the pyrolysis gasoline model.

3.2.1. Configuration 1

First, the simulation of the extraction process using the configuration 1 was performed. As explained previously, this configuration is composed of a countercurrent extraction column and a recovery section formed by a flash distillation (Fig. 1). The simulations were performed using a solvent to feed (S/F) ratio in mass of 5.0 and using the {[4empy][NTf$_2$] + [emim][DCA]} binary IL-IL mixture with [4empy][NTf$_2$] contents of 0, 25, 50, 75, and 100 wt. %. We have chosen a S/F ratio of 5.0 because this value was the optimal in the experimental extraction of BTX from pyrolysis gasoline using the IL mixture proved in this work [8].

The performance of the IL-based solvents in the dearomatization of the pyrolysis gasoline were analyzed by process simulations attending to aromatic recovery, aromatic purity in the product stream and aliphatic purity in the raffinate stream in mass units. These three variables are depicted in Fig. 12 as a function of the wt. % [4empy][NTf$_2$] in the IL mixture employing the Configuration 1. The composition in the IL mixture had a significant effect on the values of recoveries and purities. An increase in the [4empy][NTf$_2$] content in the mixture caused a rise in aromatic recovery and aliphatic purity in the raffinate. This trend can be explained considering the liquid-liquid equilibrium data obtained in the extraction of toluene from *n*-heptane using the [4empy][NTf$_2$] and [emim][DCA] pure ILs. The [4empy][NTf$_2$] exhibited a higher mass-based toluene distribution ratio (0.265) [45] than the [emim][DCA] (0.155) [37];

for that reason, the aromatic recovery and the purity of the aliphatics in the raffinate increased with the [4empy][NTf_2] content in the mixture.

The aromatic purity is related to the values of selectivity exhibited by the solvent. The decrease in the aromatic purity with the wt. % [4empy][NTf_2] in the IL mixture observed in Fig. 12 is consistent with the higher toluene/*n*-heptane selectivity (71.2) exhibited by the [emim][DCA] [37] with respect to that of [4empy][NTf_2] (29.5) [45]. Because of this, the purity of the extracted aromatic hydrocarbons decreased with the [4empy][NTf_2] content in the solvent.

Therefore, the most adequate composition of the IL mixture must be chosen to ensure high values of aromatic recovery and purity. As can be inferred from Fig. 12, the almost complete recovery of the aromatic hydrocarbons could be achieved using the {[4empy][NTf_2] + [emim][DCA]} mixture with % [4empy][NTf_2] higher than 75 %. However, the values of aromatic purity would be lower than 89 % using these IL-based solvents.

The effect of the composition in the IL mixture on the energy requirements of the proposed process in Configuration 1 has been also studied. In Table 5, heat, cooling and total energy needs as a function of the % [4empy][NTf_2] in the IL mixture are reported. To analyze the effect of the composition of the IL mixture on the energy needs is important to keep in mind the mass-based specific heats of the ILs forming the mixture: [emim][DCA] (1.87 $kJ \cdot kg^{-1} \cdot K^{-1}$) and [4empy][$NTf_2$] (1.60 $kJ \cdot kg^{-1} \cdot K^{-1}$) at 313.2 K [43]. According to the higher specific heat of the [emim][DCA], the energy needs should decrease with the % [4empy][NTf_2] in the mixture. Nevertheless, a minimum of energy requirements is observed at a 25-50 wt. % of [4empy][NTf_2] in the mixture in Table 5. This is because the amount of extracted hydrocarbon also affects the energy needs of Configuration 1, since the heating needs in the heat exchanger E-102 and cooling needs in the E-103 heat exchanger are function of the extract stream flow. As the [4empy][NTf_2] exhibited higher capacity to extract aromatic hydrocarbons from the pyrolysis gasoline and lower heat capacity than the [emim][DCA], two opposite effects are present in the calculation of the energy needs as a function of the composition in the IL mixture. Because of this, a minimum in the total energy needs was observed at intermediate compositions of [4empy][NTf_2] in the mixture. Therefore, tuning the binary IL-IL mixtures composition allows enhancing not only separation efficiency but also the energy requirements of the extraction process.

3.2.2. Configuration 2

To increase the obtained aromatic purity, the recovery section will be formed in Configurations 2 and 3 by two or three flash distillations, to selectively evaporate the aliphatic

compounds from the solvent and to obtain a final product stream with a higher aromatic purity. Configuration 2 (Fig. 2) was tested to evaluate the effect of a second flash distillation in the recovery section on the values of aromatic purity, aromatic recovery, aliphatic purity and energy needs. In Fig. 13, purities and recoveries obtained in the simulation of Configuration 2 as a function of composition of the IL mixture are plotted. As in Configuration 1, an increase in the aromatic recovery and aliphatic purity was observed with the percentage of [4empy][NTf_2] in the mixture and the aromatic purity exhibited the opposite trend. However, the obtained aromatic purity was significantly higher than that obtained using Configuration 1. For instance, employing the [4empy][NTf_2] as solvent, the aromatic purity in the previous configuration was 79.5 % whereas in Configuration 2 was 86.6 %. Moreover, the employment of two flash distillations has increased the purity of the extracted hydrocarbons without affecting the aromatic recovery. In Configuration 1, an IL mixture with a 75 % [4empy][NTf_2] allows obtaining an almost complete recovery of the aromatic hydrocarbons with an aromatic purity of 89.1 %. In Configuration 2, the aromatic recovery using this IL mixture has barely changed but the aromatic purity has increased to 92.5 %.

Heat needs for Configuration 2 as a function of composition in the IL mixture are reported in Table 5. As discussed previously, the lowest value of total energy needs was obtained employing the IL mixture with a 50 % of each IL. Comparing the energy requirements of Configuration 2 with those of Configuration 1 a slight decrease of heat and cooling needs was observed. The heating needs were lower in Configuration 2 because of the significant amount of hydrocarbons recycled to the column in the vapor stream obtained in the first flash and, therefore, the flow of the stream heated to 393.2 K in the heat exchanger E-102 is lower in Configuration 2. The recycled stream also affects the cooling needs because the recycled hydrocarbons in the first flash are cooled from 333.2 K to 313.2 K whereas in Configuration 1 all the extracted hydrocarbons were cooled from 393.2 K to 313.2 K after the flash distillation. Thus, employing a second flash distillation has decreased the energy requirements of the extraction process and increased the purity of the extracted hydrocarbons. Nevertheless, the values of aromatic purity (86-96 %) obtained in this configuration are not high enough to obtain significant income from selling the aromatic product.

3.2.3. Configuration 3

A new configuration of the recovery section formed by three flash distillations and a S/F ratio of 7.0 was tested in Configuration 3 (Fig. 3). The value of S/F ratio has been increased with respect to the previous configurations (S/F=5.0) because this configuration includes three

recycle loops and a higher solvent flow is required. The influence of the configuration on the S/F ratio is more deeply studied in the section 3.3.

In Configuration 3, the first flash distillation operates at 333.2 K and 300 mbar as in the Configuration 2. The aim of the second flash distillation is selectively recover more aliphatic hydrocarbons from the IL-based solvent to increase the aromatic purity. For this reason, this flash operates at 333.2 K and 200 mbar, since the aliphatic/aromatic relative volatilities in the presence of ILs decreases as the temperature rises [9]. The operating conditions of the third flash are coincident with the employed in the two previous configurations: 393.2 K and 10 mbar.

Aromatic recoveries and purities and aliphatic purities in the raffinate using the {[4empy][NTf_2] + [emim][DCA]} mixture in Configuration 3 are depicted in Fig. 14. The influence of the mixture composition on the three calculated parameters was the same previously discussed in Configuration 1. An aromatic recovery higher than 99.7 % could be obtained employing IL mixtures with % [4empy][NTf_2] higher than 75 %. Analyzing the values of the aromatic purity, the {[4empy][NTf_2] (75 %) + [emim][DCA] (25 %)} binary IL-IL mixture seems to be the adequate composition to achieve high aromatic purities with an almost complete aromatic recovery. The aromatic purity obtained with this composition in Configuration 3 (96.7 %) is substantially higher than that obtained in Configuration 1 and 2. Therefore, the addition of a third flash distillation to the process has been useful to increase the purity of the obtained aromatic hydrocarbons.

In Table 5, the energy requirements for Configuration 3 are listed together with the values for Configuration 1 and 2. As a result of the higher S/F ratio used in Configuration 3, heat and cooling needs of this configuration were considerably higher than those of the previous configurations. The higher impact of the S/F ratio on the energy needs was in the 1-way heat exchanger E-100 because the solvent is cooled from 393.2 K to 313.2 K and in the heat exchanger E-102 in which the extract stream is heated from 333.2 K to 392.2 K.

The effect of the IL mixture composition on the energy requirements is similar to those discussed for Configurations 1 and 2. In Configuration 3, the {[4empy][NTf_2] (75 %) + [emim][DCA] (25 %)} IL mixture has exhibited the lowest total energy needs. The use of this composition in the IL mixture implied lower energy requirements in the three configurations than those for the pure [4empy][NTf_2]. In addition, higher aromatic purities and similar aromatic recoveries and aliphatic purities in the raffinate were achieved for the {[4empy][NTf_2] (75 %) + [emim][DCA] (25 %)} mixture than those employing the [4empy][NTf_2]. Therefore, this composition was selected as the most adequate to be employed in the extraction of aromatic hydrocarbons from pyrolysis gasoline. Then, the study

of the effect of S/F ratio in the three configurations was made employing the IL mixture with its most adequate composition as solvent.

3.3. Effect of the solvent-to-feed ratio using the {[4empy][NTf_2] (75 %) + [emim][DCA] (25 %)} binary IL-IL mixture

The simulation of Configuration 1 using the {[4empy][NTf_2] (75 %) + [emim][DCA] (25 %)} IL mixture was performed at S/F ratios from 3.0 to 7.0 to determine the most suitable value of this variable. In Fig. 15, aromatic purities, aromatic recoveries, and aliphatic purities as a function of S/F ratio are depicted. As expected, an increase in the S/F ratio caused a rise in aromatic recovery and aliphatic purity but the aromatic purity decreased because of the greater amount of extracted aliphatic hydrocarbons. To ensure an aromatic recovery higher than the 99 %, a S/F ratio greater than 5.0 should be employed in Configuration 1. At S/F ratios of 3.0 and 4.0, the solvent flow is not enough to dissolve the most of the aromatic hydrocarbons, observing a significant decrease in aromatic recovery and aliphatic purity in the raffinate. Hence, the value of 5.0 seems to be the optimal because higher S/F ratios would imply larger energy consumptions and lower aromatic purities. The recoveries and purities and total energy needs for Configuration 1 using the optimal S/F ratio are listed in Table 6 in order to be compared with the results obtained in the optimization of Configurations 2 and 3. In Table S3 of the Supplementary Material, material and energy balances using a S/F ratio of 5.0 in Configuration 1 are listed.

Results obtained in the optimization of the S/F ratio in the Configuration 2 are plotted in Fig. 16. Aromatic recoveries larger than 99.5 % were achieved at S/F mass ratios higher than 5.0. This value of S/F ratio was selected as the optimal to ensure high aromatic purities in the product stream. In Table 6, aromatic purity and recovery, aliphatic purity in the raffinate streams and total energy needs for Configuration 2 are reported. As can be observed, the optimized Configuration 2 achieved an aromatic purity significantly higher than Configuration 1. However, the second flash distillation caused a slight decrease of the aromatic recovery and the aliphatic purity in the raffinate due to the important content of aromatic hydrocarbons in the recycled stream from the second flash to the extraction column. By contrast, energy requirements were lower in Configuration 2 with respect to Configuration 1 because the recycled hydrocarbons obtained in the vapor stream of the first flash distillation are heated to 333.2 K instead of 393.2 K. Temperatures, pressures, flows, compositions, and enthalpies of the streams forming the Configuration 2 at a S/F ratio of 5.0 are summarized in the Table S4 of the Supplementary Material.

Finally, the S/F mass ratio employed in the Configuration 3 was also optimized. As discussed previously, as a result of the three recycled streams, the S/F ratio needed in this configuration is higher than those in Configurations 1 and 2. For that reason, the optimization was performed at S/F mass ratios between 5.0 and 9.0, showing the results in the Fig. 17. As observed, employing a S/F ratio higher than 6.5 almost a complete recovery of aromatic hydrocarbons from the pyrolysis gasoline could be obtained. At S/F ratios lower than 6.5 a noticeable decrease in the aromatic purity and aromatic recovery was observed, whereas the purity of the obtained aromatics decreased at S/F ratios greater than 6.5. Thus, the optimal S/F mass ratio for the Configuration 3 was 6.5. In the Table S5 of the Supplementary Material, material and energy balances at a S/F ratio of 6.5 for the Configuration 3 are listed. Purities, aromatic recovery, and total energy needs employing the optimized configuration are also shown in Table 6. As may be seen in this table, the aromatic purity employing Configuration 3 was higher than using Configurations 1 or 2. Furthermore, the values of the aromatic recovery and aliphatic purity in the raffinate were greater than the 98 % fixed by Meindersma et al. (2008) in the simulation of the extraction process of aromatic hydrocarbons using the [4bmpy][BF_4] [3]. The most important drawbacks of Configuration 3 with respect to Configurations 1 and 2 are the energy consumption and the required solvent flow. Still, the purity of the obtained aromatic hydrocarbons, 97.7 wt. % in this case, is essential to simplify and reduce the cost of the subsequent purification steps and to increase the income from selling the high grade aromatic hydrocarbons.

4. Conclusions

The extraction process of aromatic hydrocarbons from pyrolysis gasoline using the {[4empy][NTf_2] + [emim][DCA]} IL mixture was simulated using an a priori COSMO-based/Aspen Plus integrated tool. Predictions of liquid-liquid equilibria, vapor-liquid equilibria and physical properties of the solvents were successfully validated by a comparative analysis with experimental results from literature. In the process simulations, three configurations with one, two, or three flash distillations in the recovery section were evaluated. In addition, the effect of the composition in the IL mixture on the aromatic recovery, purity and energy need was also studied. From the results obtained in the simulations, the binary IL-IL mixture with a 75 % of [4empy][NTf_2] was selected as the most adequate composition to ensure high values of aromatic recoveries and purities. Finally, the S/F ratio in the three proposed configuration was optimized using the {[4empy][NTf_2] (75 %) + [emim][DCA] (25 %)} as solvent. The configuration formed by three flash distillations has exhibited the best performance with a S/F mass ratio of 6.5, obtaining an aromatic recovery of

99.8 %, an aromatic purity of 97.7 % and an aliphatic purity in the raffinate of 99.5 %. In conclusion, the COSMO-based/Aspen Plus methodology has been successfully employed to simulate the entire process of extraction from pyrolysis gasoline and recovery of the extracted hydrocarbons from the IL mixture, allowing introducing new technical criteria to select the solvent with more adequate properties. This methodology could be applied in the simulation of other separation processes employing IL mixtures to select the most adequate composition in the mixture and to evaluate the viability of several configurations to achieve the separation.

Acknowledgments

The authors are grateful to Ministerio de Economía y Competitividad (MINECO) of Spain for financial support of Projects CTQ2014-52288-R and CTQ2014–53655-R and to Comunidad Autónoma de Madrid for the Project S2013/MAE-2800. Noemí Delgado-Mellado also thanks MINECO for awarding them an FPI grant (Reference BES–2015–072855) and Marcos Larriba also thanks MINECO for awarding him a Juan de la Cierva-Formación Contract (Reference FJCI-2015-25343). Pablo Navarro thanks Fundação para a Ciência e a Tecnologia for awarding him a postdoctoral grant (Reference SFRH/BPD/117084/2016). We are very grateful to Centro de Computación Científica de la Universidad Autónoma de Madrid for computational facilities.

References

[1] H.G. Franck, J.W. Staldelhofer, Industrial Aromatic Chemistry; Springer–Verlag: Berlin, 1988.

[2] J. Gary, G. Handwerk, M. Kaiser, Petroleum Refining Technology and Economics, 5th ed.; CRC Press: Boca Raton, FL, 2007.

[3] G.W. Meindersma, A.B. de Haan, Conceptual Process Design for Aromatic/aliphatic Separation with Ionic Liquids. Chem. Eng. Res. Des. 86 (2008) 745–752.

[4] R.I. Canales, J.F. Brennecke, Comparison of ionic liquids to conventional organic solvents for extraction of aromatics from aliphatics. J. Chem. Eng. Data 61 (2016) 1685-1699.

[5] G.W. Meindersma, A.R. Hansmeier, A.B. de Haan, Ionic liquids for aromatics extraction. Present status and future outlook, Ind. Eng. Chem. Res. 49 (2010) 7530–7540.

[6] C.D. Wilfred, C.F. Kiat, Z. Man, M. A. Bustam, M.I.M. Mutalib, C. Z. Phak, Extraction of dibenzothiophene from dodecane using ionic liquids, Fuel Process. Technol. 93

(2012) 85–89.

[7] M. Larriba, P. Navarro, E.J. González, J. García, F. Rodríguez, Separation of BTEX from a naphtha feed to ethylene crackers using a binary mixture of [4empy][Tf2N] and [emim][DCA] ionic liquids, Sep. Purif. Technol. 144 (2015) 54−62.

[8] M. Larriba, P. Navarro, E.J. González, J. García, F. Rodríguez, Dearomatization of pyrolysis gasolines from mild and severe cracking by liquid–liquid extraction using a binary mixture of [4empy][Tf2N] and [emim][DCA] ionic liquids, Fuel Process. Technol. 137 (2015) 269–282.

[9] P. Navarro, M. Larriba, J. García, E.J. González, F. Rodríguez, Vapor–liquid equilibria of {n-heptane + toluene + [emim][DCA]} system by headspace gas chromatography, Fluid Phase Equilib. 387 (2015) 209−216.

[10] M. Larriba, P. Navarro, J. García, F. Rodríguez, Separation of toluene from n-heptane, 2,3-dimethylpentane, and cyclohexane using binary mixtures of [4empy][Tf2N] and [emim][DCA] ionic liquids as extraction solvents, Sep. Purif. Technol. 120 (2013) 392−401.

[11] M. Larriba, P. Navarro, J. García, F. Rodríguez, Liquid-liquid extraction of toluene from n-alkanes using {[4empy][Tf2N] + [emim][DCA]} ionic liquid mixtures, J. Chem. Eng. Data 59 (2014) 1692–1699.

[12] A.M. Pinto, H. Rodríguez, Y.J. Colón, A. Arce Jr., A. Arce, A. Soto, Absorption of Carbon Dioxide in Two Binary Mixtures of Ionic Liquids, Ind. Eng. Chem. Res. 52 (2013) 5975–5984.

[13] W. Li, Y. Liu, L. Wang, G. Gao, Using Ionic Liquid Mixtures To Improve the SO2 Absorption Performance in Flue Gas, Energy Fuels 31 (2017) 1771–1777.

[14] H. Niedermeyer, J.P. Hallet, I.J. Villar-Garcia, P.A. Hunt, T. Welton, Mixtures of ionic liquids, Chem. Soc. Rev. 41 (2012) 7780–7802.

[15] M.T. Clough, C.R. Crick, J. Grasvik, P.A. Hunt, H. Niedermeyer, T. Welton, O.P. Whitaker, A physicochemical investigation of ionic liquid mixtures, Chem. Sci. 6 (2015) 1101–1114.

[16] G. Chatel, J.F.B. Pereira, V. Debbeti, H. Wang, R. Rogers, Mixing ionic liquids – “simple mixtures” or “double salts”?, Green Chem. 16 (2014) 2051−2083.

[17] S. Omar, J. Lemus, E. Ruiz, V.R. Ferro, J. Ortega, J. Palomar, Ionic liquid mixtures - An analysis of their mutual miscibility, J. Phys. Chem. B 118 (2014) 2442−2450.

[18] R. Anantharaj, T. Banerjee, COSMO-RS based predictions for the desulphurization of diesel oil using ionic liquids: Effect of cation and anion combination, Fuel Process. Technol. 92 (2011) 39–52.

[19] A.R. Ferreira, M.G. Freire, J.C. Ribeiro, F.M. Lopes, J.G. Crespo, J.A.P. Coutinho, Overview of the liquid-liquid equilibria of ternary systems composed of ionic liquid and aromatic and aliphatic hydrocarbons and their modeling by COSMO-RS, Ind. Eng. Chem. Res. 51 (2012) 3483–3507.

[20] Y. Bai, R. Yan, F. Huo, J. Qian, X. Zhang, S. Zhang, Recovery of methacrylic acid from dilute aqueous solutions by ionic liquids though hydrogen bonding interaction, Sep. Purif. Technol. 184 (2017) 354−364.

[21] X. Li, S.R.A. Kersten, B. Schuur, Extraction of acetic acid, glycolaldehyde and acetol from aqueous solutions mimicking pyrolysis oil cuts using ionic liquids, Sep. Purif. Technol. 175 (2017) 498−505.

[22] U. Domanska, M. Wazlo, Kamil Paduszynski, Extraction of butan-1-ol from aqueous solution using ionic liquids: An effect of cation revealed by experiments and thermodynamic models, Sep. Purif. Technol. (2017), http://dx.doi.org/10.1016/j.seppur.2017.05.056

[23] M. Larriba, P. Navarro, M. Gonzalez-Miquel, S. Omar, J. Palomar, J. García, F. Rodríguez, Dicyanamide-based Ionic Liquids in the Liquid-Liquid Extraction of Aromatics from Alkanes: Experimental Evaluation and Computional Predictions, Chem. Eng. Res. Des. 109 (2016) 561–572.

[24] V.R. Ferro, E. Ruiz, J. de Riva, J. Palomar, Introducing process simulation in ionic liquids design/selection for separation processes based on operational and economic criteria through the example of their regeneration. Sep. Purif. Technol. 97 (2012) 195–204.

[25] J. de Riva, V.R. Ferro, D. Moreno I. Díaz, J. Palomar, Aspen Plus supported conceptual design of the aromatic–aliphatic separation from low aromatic content naphtha using 4-methyl-N-butylpyridinium tetrafluoroborate ionic liquid. Fuel Process. Technol. 146 (2016) 29–38.

[26] V.R. Ferro, E. Ruiz, M. Tobajas, J.F. Palomar, Integration of COSMO-based methodologies into commercial process simulators: separation and purification of reuterin, Aiche J. 58 (2012) 3404–3415.

[27] E. Ruiz, V.R. Ferro, J. de Riva, D. Moreno, J. Palomar, Evaluation of ionic liquids as absorbents for ammonia absorption refrigeration cycles using COSMO-based process simulations, Appl. Energy 123 (2014) 281–291.

[28] J. Bedia, E. Ruiz, J. de Riva, V.R. Ferro, J. Palomar, J.J. Rodriguez, Optimized ionic liquids for toluene absorption, Aiche J. 59 (2013) 1648–1656.

[29] V.R. Ferro, J. de Riva, D. Sánchez, E. Ruiz, J. Palomar, Conceptual design of unit

operations to separate aromatic hydrocarbons from naphtha using ionic liquids. COSMO-based process simulations with multi-component “real” mixture feed, Chem. Eng. Res. Des. 94 (2015) 632–647.

[30] J. de Riva; J. Suárez-Reyes, D. Moreno, I. Díaz, V. Ferro, J. Palomar, Ionic liquids for post-combustion CO2 capture by physical absorption: Thermodynamic, kinetic and process analysis. Int. J. Greenh. Gas Con. 61 (2017) 61−70.

[31] P. García-Gutiérrez, J. Jacquemin, C. McCrellis, I. Dimitriou, S. F. Rebecca Taylor, C. Hardacre, R.W.K. Allen, Techno-economic feasibility of selective CO_2 capture processes from biogas streams using ionic liquids as physical absorbents, Energy Fuels 30 (2016) 5052−5064.

[32] S.T. Anjan, Ionic liquid for aromatic extraction: are they ready? Chem. Eng. Prog. 102 (2006) 30–39.

[33] P. Navarro, M. Larriba, J. García, F. Rodríguez, Design of the recovery section of the extracted aromatics in the separation of BTEX from naphtha feed to ethylene crackers using [4empy][Tf2N] and [emim][DCA] mixed ionic liquids as solvent, Sep. Purif. Technol. 180 (2017) 149−156.

[34] A. Schäfer, A. Klamt, D. Sattel, J. Lohrenz, F. Eckert, COSMO implementation in TURBOMOLE: extension of an efficient quantum chemical code towards liquid systems, Phys. Chem. Chem. Phys. 2 (2000) 2187–2193.

[35] A. Klamt, COSMO-RS: From Quantum Chemistry to Fluid Phase Thermodynamics and Drug Design, first ed. Elsevier, Amsterdam, 2005.

[36] F. Eckert, A. Klamt, 2014. COSMOtherm, Release 12.01 Version C3.0 ed.COSMOlogic GmbH & Co. KG, Leverkusen, Germany.

[37] M. Larriba, P. Navarro, J. García, F. Rodríguez, Liquid-liquid extraction of toluene from heptane using [emim][DCA], [bmim][DCA], and [emim][TCM] ionic liquids, Ind. Eng. Chem. Res. 52 (2013) 2714−2720.

[38] J. de Riva, V.R. Ferro, L. del Olmo, E. Ruíz, R. López, J. Palomar, Statistical Refinement and Fitting of Experimental Viscosity-to-Temperature Data in Ionic Liquids. Ind. Eng. Chem. Res 53 (2014) 10475–10484.

[39] https://esupport.aspentech.com/S_Article?id=000045549

[40] Aspen Physical Property System. Physical Property Models. Version Number V7.3.2. Aspen Tech, Cambridge, 2012.

[41] G.W. Meindersma, A.B. de Haan, Cyano-containing ionic liquids for the extraction of aromatic hydrocarbons from an aromatic/aliphatic mixture, Sci. China Chem 55 (2012) 1488−1499.

[42] G.W. Meindersma, A.J.G. Podt, A.B. de Haan, Selection of Ionic Liquids for the Extraction of Aromatic Hydrocarbons from Aromatic/aliphatic Mixtures, Fuel Process. Technol. 87 (2005) 59–70.

[43] P. Navarro, M. Larriba, J. García, F. Rodríguez, Thermal stability, specific heats, and surface tensions of ([emim][DCA] + [4empy][Tf_2N]) ionic liquid mixtures, J. Chem. Thermodyn. 76 (2014) 152–160.

[44] P. Navarro, M. Larriba, J. García, F. Rodríguez, Vapor-liquid equilibria for *n*-heptane + (benzene, toluene, *p*-xylene, or ethylbenzene) + {[4empy][Tf_2N] (0.3) + [emim][DCA] (0.7)} binary ionic liquid mixture, Fluid Phase Equilib. 417 (2016) 41–49.

[45] J. García, S. García, J.S. Torrecilla, F. Rodríguez, Solvent extraction of toluene from heptane with the ionic liquids N–ethylpyridinium bis(trifluoromethylsulfonyl)imide and z–methyl–N–ethylpyridinium bis(trifluoromethylsulfonyl)imide (z = 2, 3 or 4) at T = 313.2 K, J. Chem. Eng. Data 55 (2010) 4937–4942.

[46] P. Navarro, M. Larriba, J. García, E.J. González, F. Rodríguez, Vapor−Liquid Equilibria of n-Heptane + Toluene +1-Ethyl-4-methylpyridinium Bis(trifluoromethylsulfonyl)imide Ionic Liquid, J. Chem. Eng. Data 61 (2016) 458−465.

[47] P. Navarro, M. Larriba, J. García, F. Rodríguez, Vapor−Liquid Equilibria for (n-Hexane, n-Octane, Cyclohexane, or 2,3-Dimethylpentane) + Toluene + {[4empy][Tf_2N] (0.3) + [emim][DCA] (0.7)} Mixed Ionic Liquids, J. Chem. Eng. Data 61 (2016) 2440−2449.

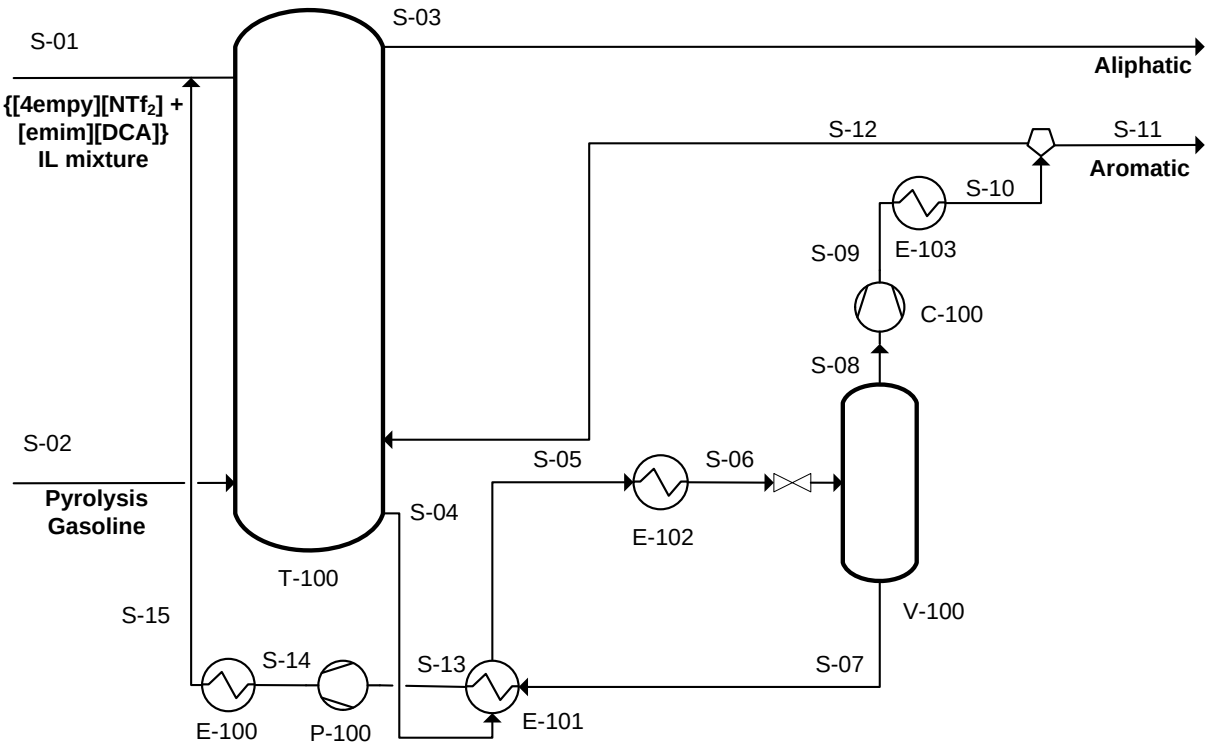

Fig. 1. Configuration 1: Flow diagram for the separation of aromatic hydrocarbons from pyrolysis gasoline using an extraction column and a flash distillation.

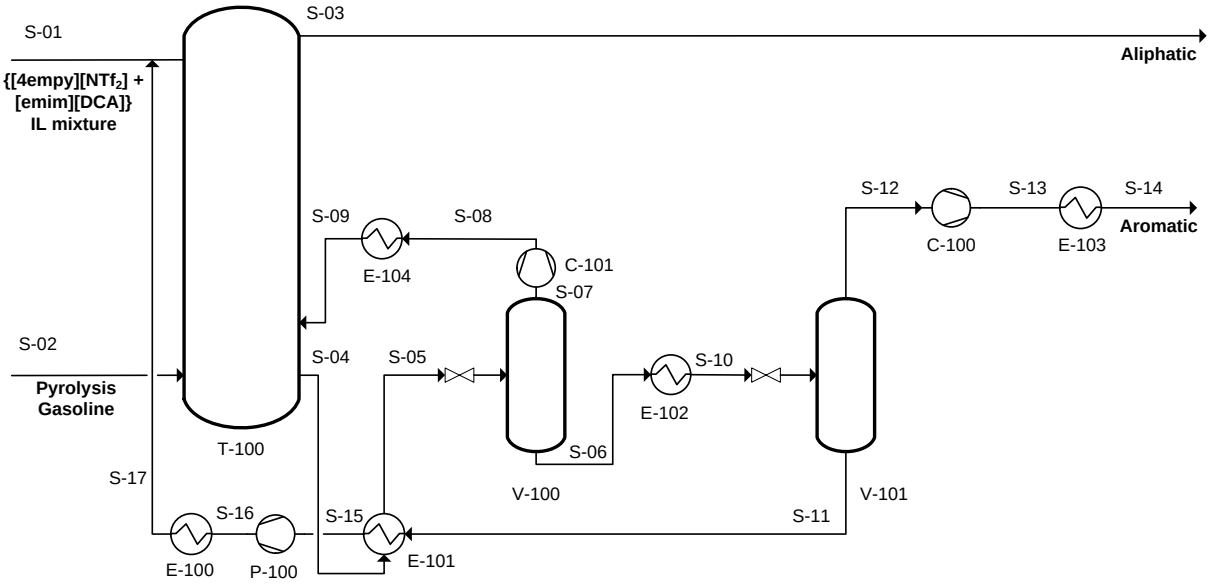

Fig. 2. Configuration 2: Flow diagram for the separation of aromatic hydrocarbons from pyrolysis gasoline using an extraction column and two flash distillations.

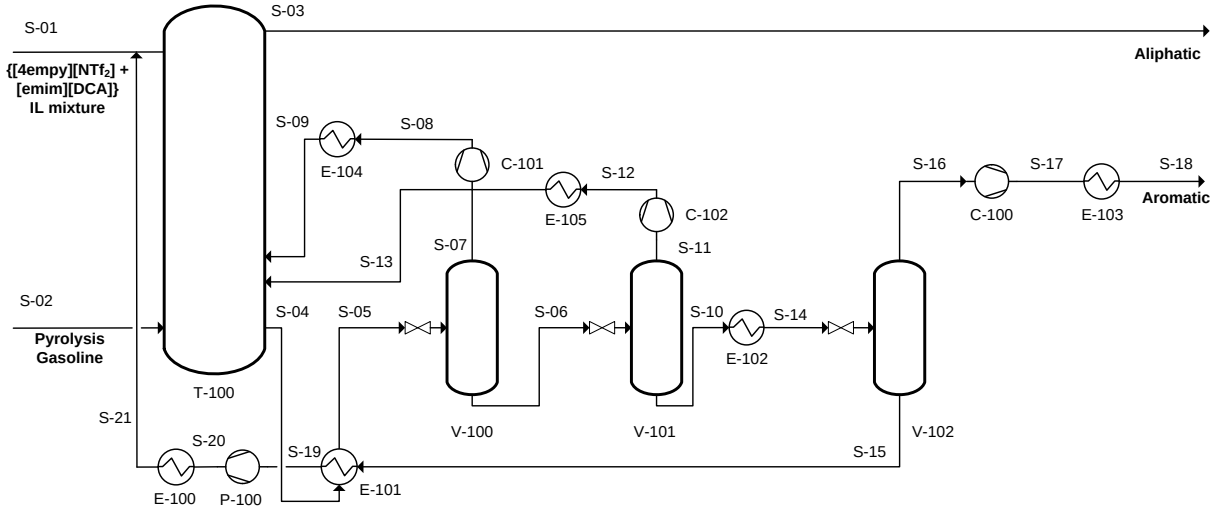

Fig. 3. Configuration 3: Flow diagram for the separation of aromatic hydrocarbons from pyrolysis gasoline using an extraction column and three flash distillations.

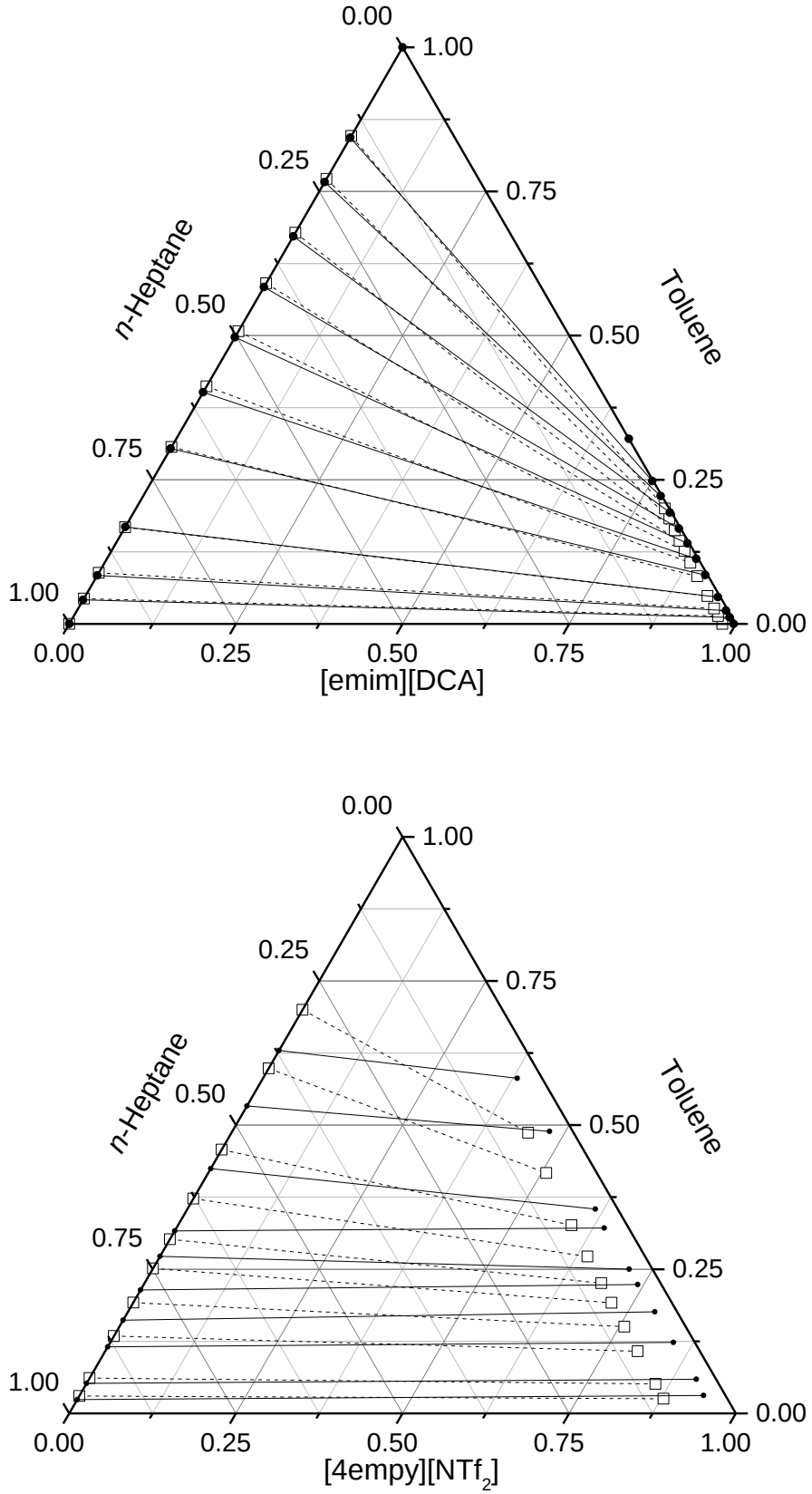

Fig. 4. Liquid-liquid equilibria at 313.2 K for the ternary systems {*n*-heptane + toluene + IL}: Experimental data [37,45] (•) and predicted data using COSMO-based method (□).

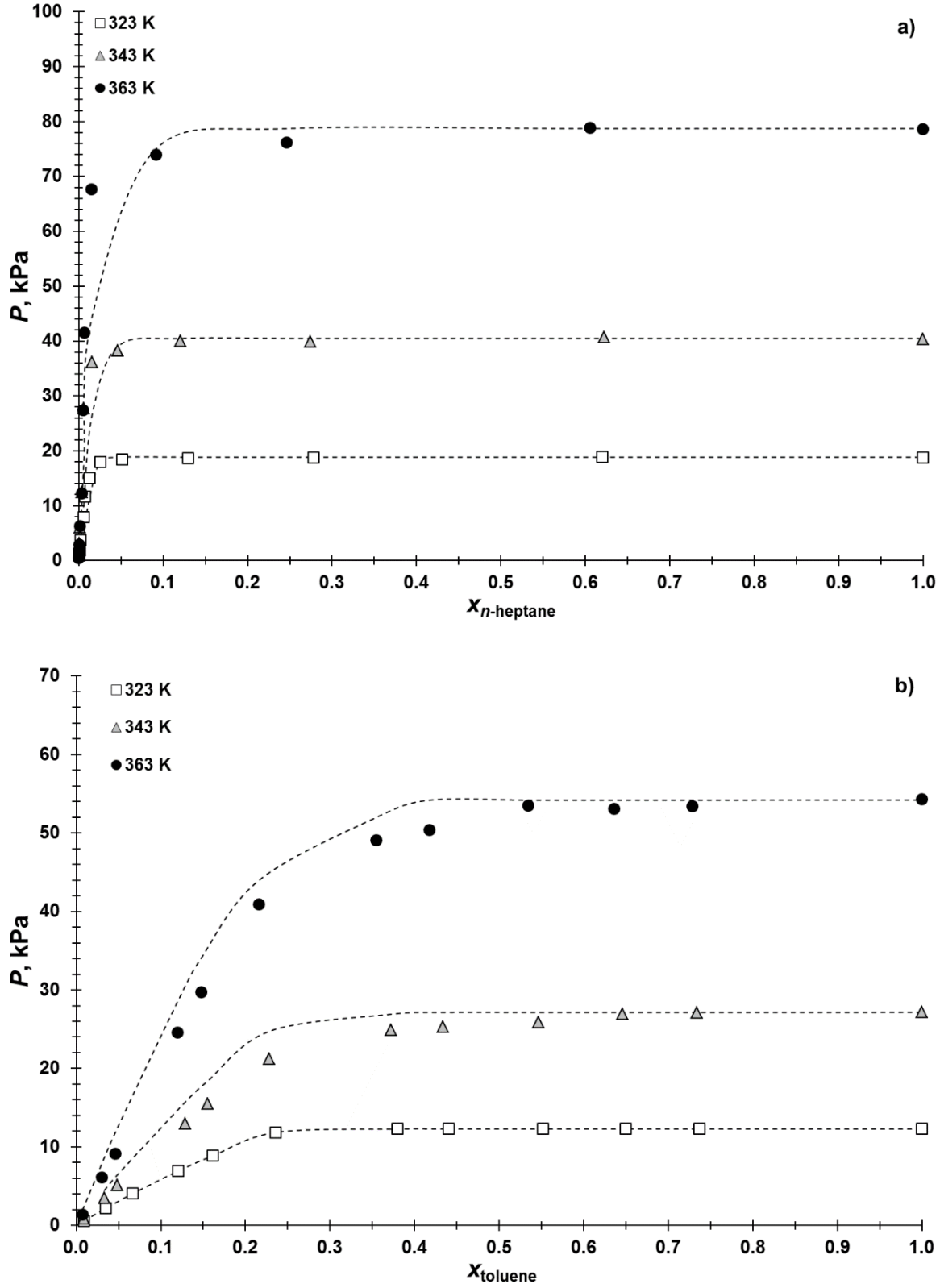

Fig. 5. Vapor-liquid equilibria for the binary systems (a), {*n*-heptane + [emim][DCA]} and (b), {toluene + [emim][DCA]}: Symbols are experimental data [9] whereas dashed lines are predicted data using COSMO-based methodology.

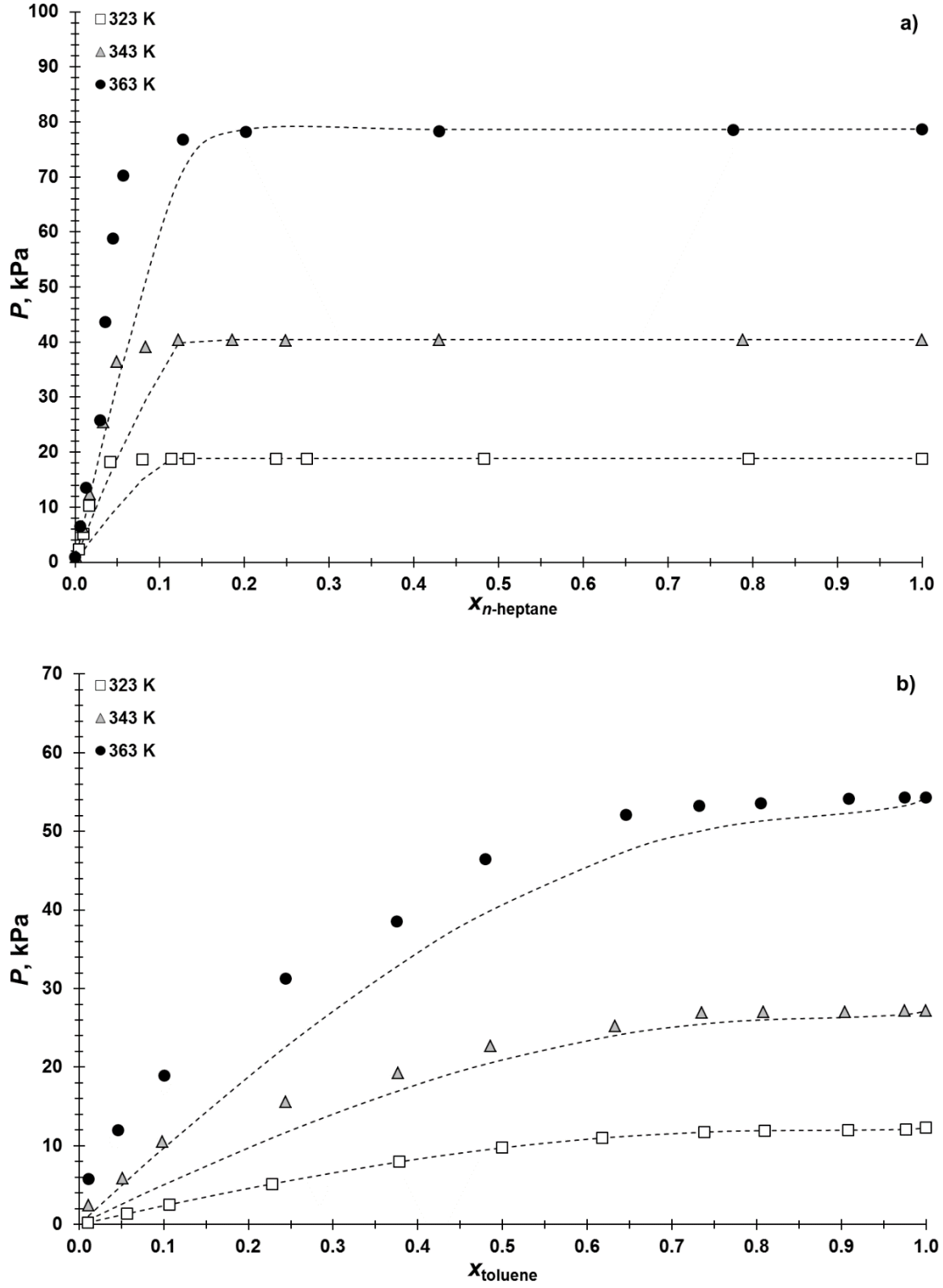

Fig. 6. Vapor-liquid equilibria for the binary systems (a), {*n*-heptane + [4empy][NTf_2]} and (b), {toluene + [4empy][NTf_2]}: Symbols are experimental data [46] whereas dashed lines are predicted data using COSMO-based methodology.

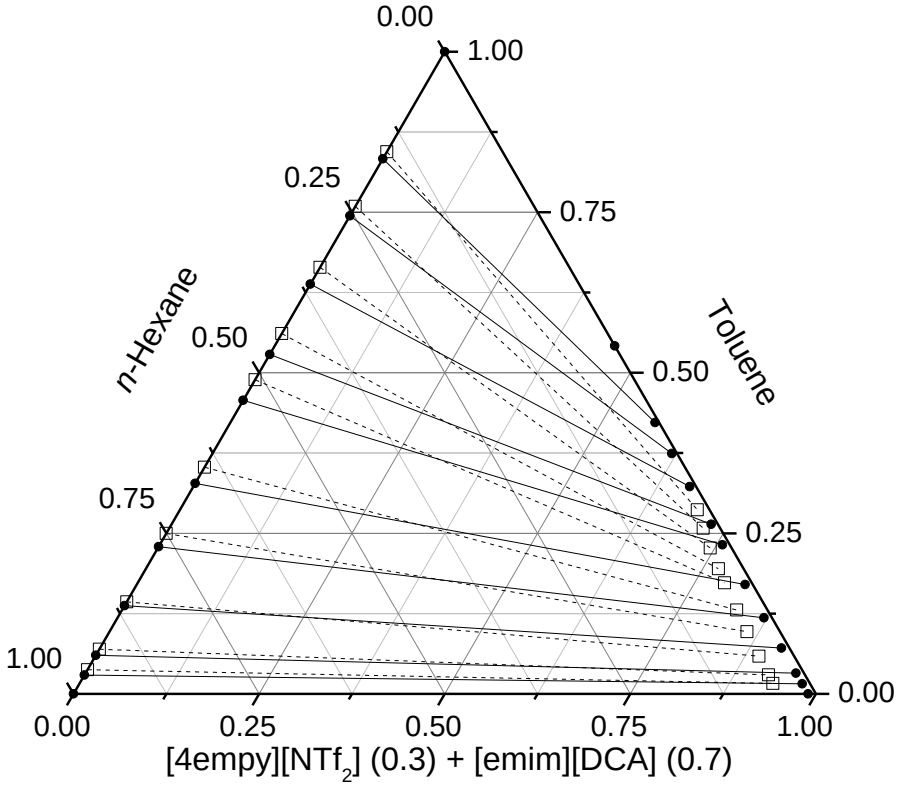
0.00
1.00
0.25
0.75
n-Hexane
0.50
Toluene
0.50
0.75
0.25
1.00
0.00
0.00
0.25
0.50
0.75
1.00
[4empy][NTf2] (0.3) + [emim][DCA] (0.7)

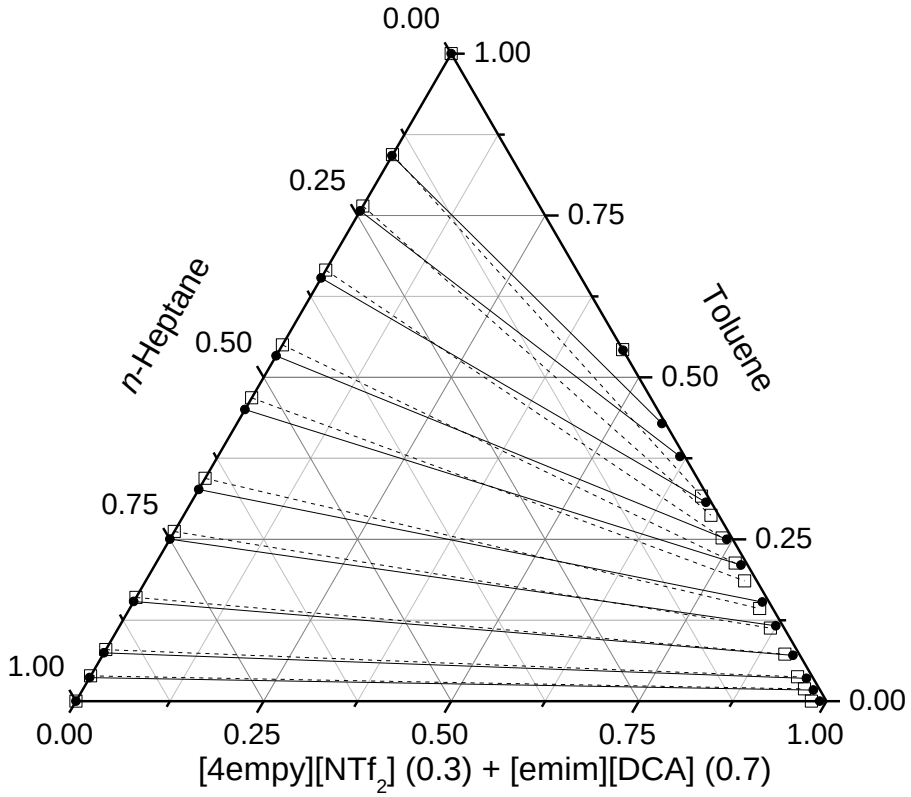
0.00
1.00
0.25
0.75
n-Heptane
0.50
Toluene
0.50
0.75
0.25
1.00
0.00
0.00
0.25
0.50
0.75
1.00
[4empy][NTf2] (0.3) + [emim][DCA] (0.7)

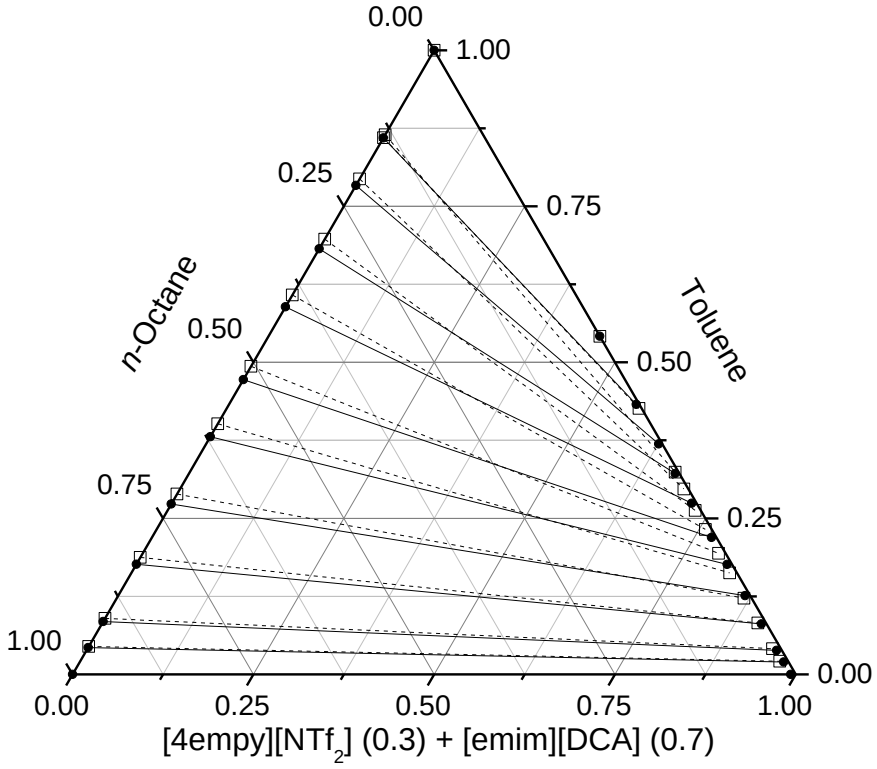

Fig. 7. Liquid-liquid equilibria at 313.2 K for the pseudoternary systems *n*-hexane, *n*-heptane, or *n*-octane + toluene + {[4empy][NTf_2] (0.3) + [emim][DCA] (0.7)}: Experimental data [10,11] (•) and predicted data using COSMO-based methodology. (□).

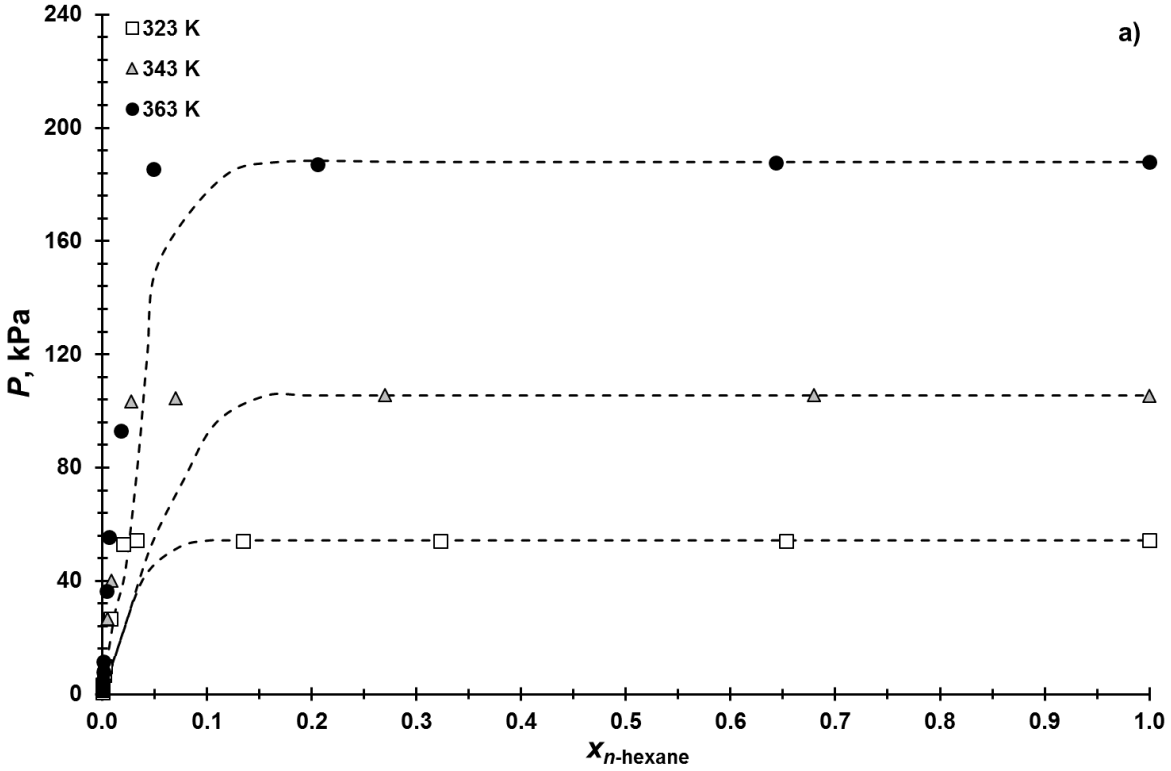
a)
323 K
343 K
363 K
P, kPa
240
200
160
120
80
40
0
0.0
0.1
0.2
0.3
0.4
0.5
0.6
0.7
0.8
0.9
1.0
x n-hexane

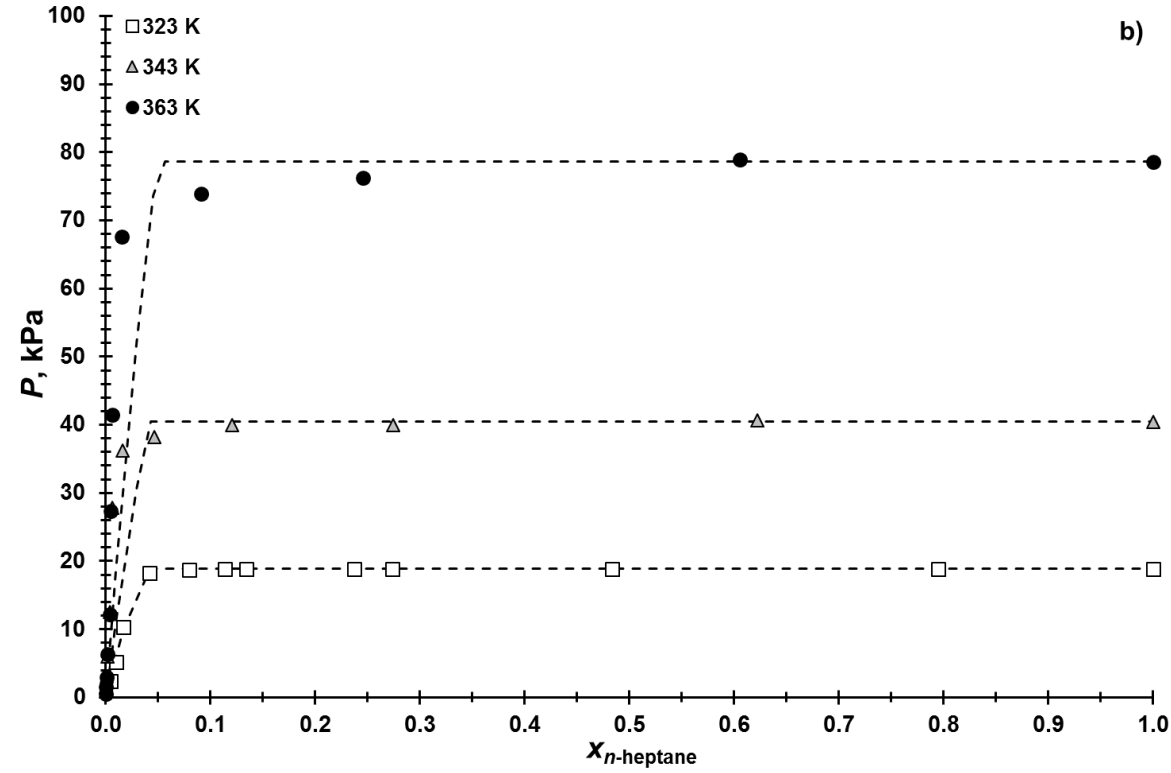
b)
323 K
343 K
363 K
P, kPa
100
90
80
70
60
50
40
30
20
10
0
0.0
0.1
0.2
0.3
0.4
0.5
0.6
0.7
0.8
0.9
1.0
x n-heptane

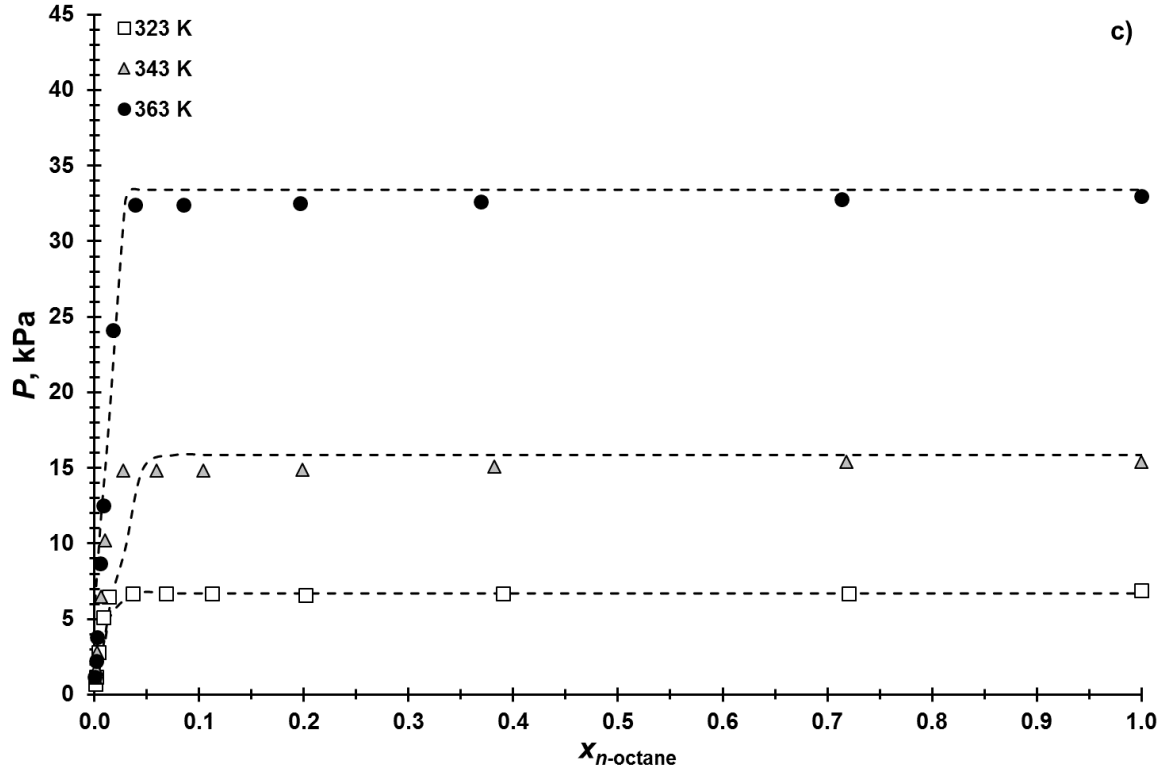

Fig. 8. Vapor-liquid equilibria for the pseudobinary systems formed by {[4empy][NTf_2] (0.3) + [emim][DCA] (0.7)} and (a), *n*-hexane; (b), *n*-heptane; (c), *n*-octane. Symbols are experimental data [44,47] whereas dashed lines are predicted data using COSMO-based methodology.

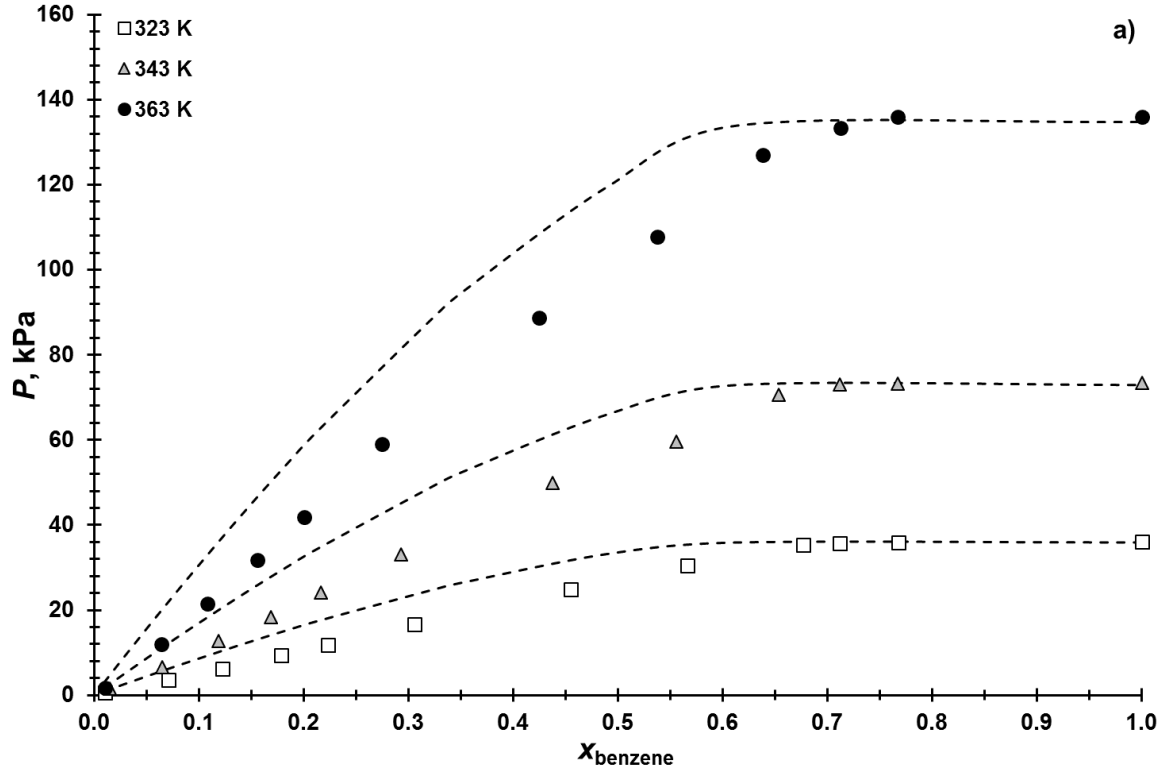
323 K
343 K
363 K
a)
P, kPa
x benzene
0
20
40
60
80
100
120
140
160
0.0
0.1
0.2
0.3
0.4
0.5
0.6
0.7
0.8
0.9
1.0

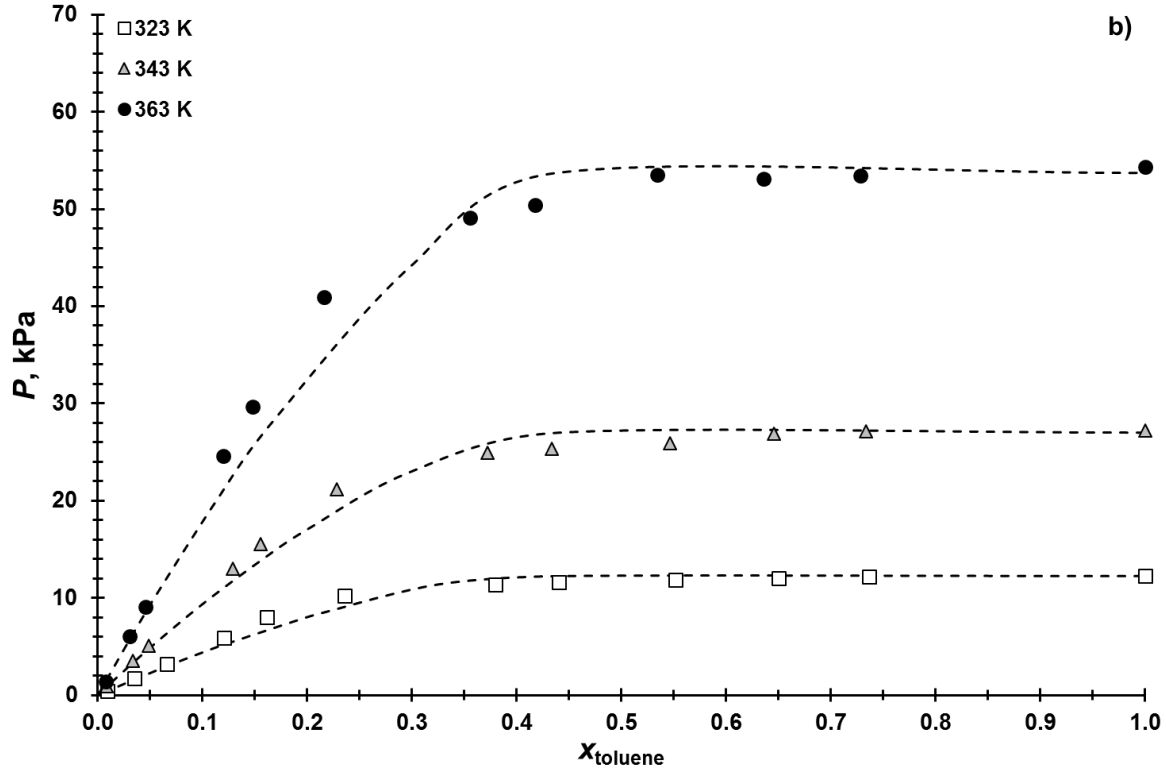
323 K
343 K
363 K
b)
P, kPa
x toluene
0
10
20
30
40
50
60
70
0.0
0.1
0.2
0.3
0.4
0.5
0.6
0.7
0.8
0.9
1.0

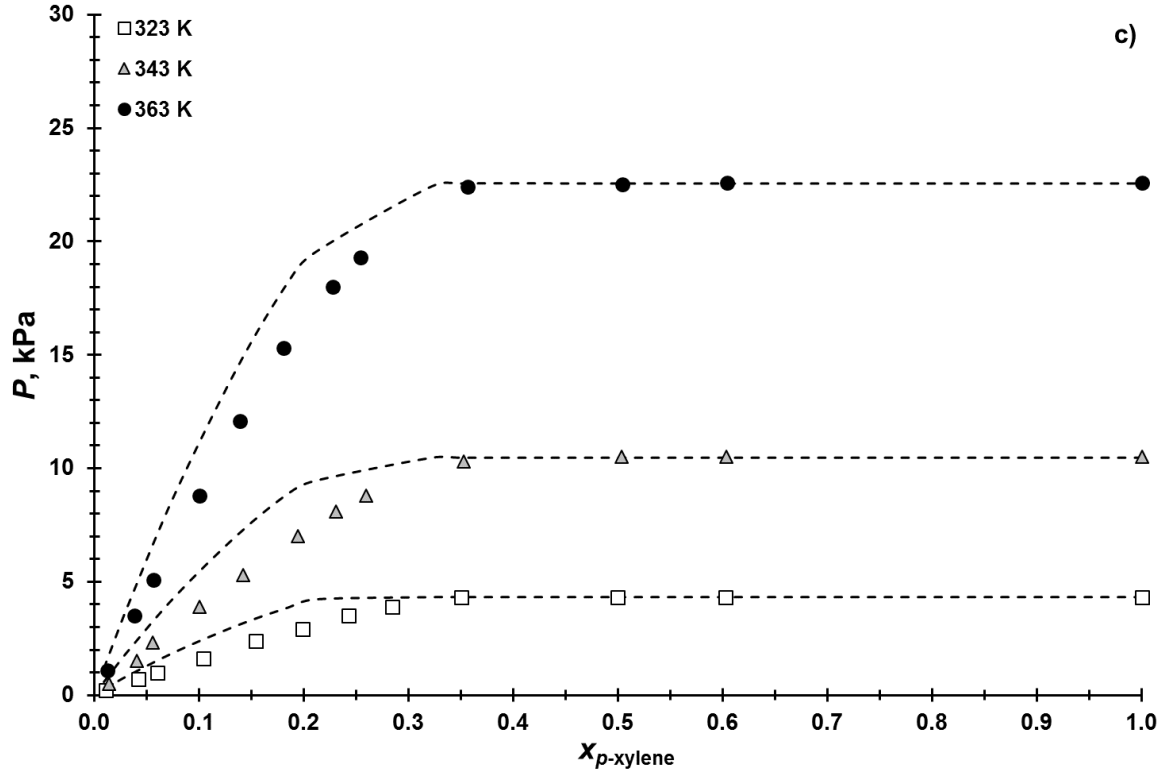

Fig. 9. Vapor-liquid equilibria for the pseudobinary systems formed by {[4empy][NTf_2] (0.3) + [emim][DCA] (0.7)} and (a), benzene; (b), toluene; (c), *p*-xylene. Symbols are experimental data [44] whereas dashed lines are predicted data using COSMO-based methodology.

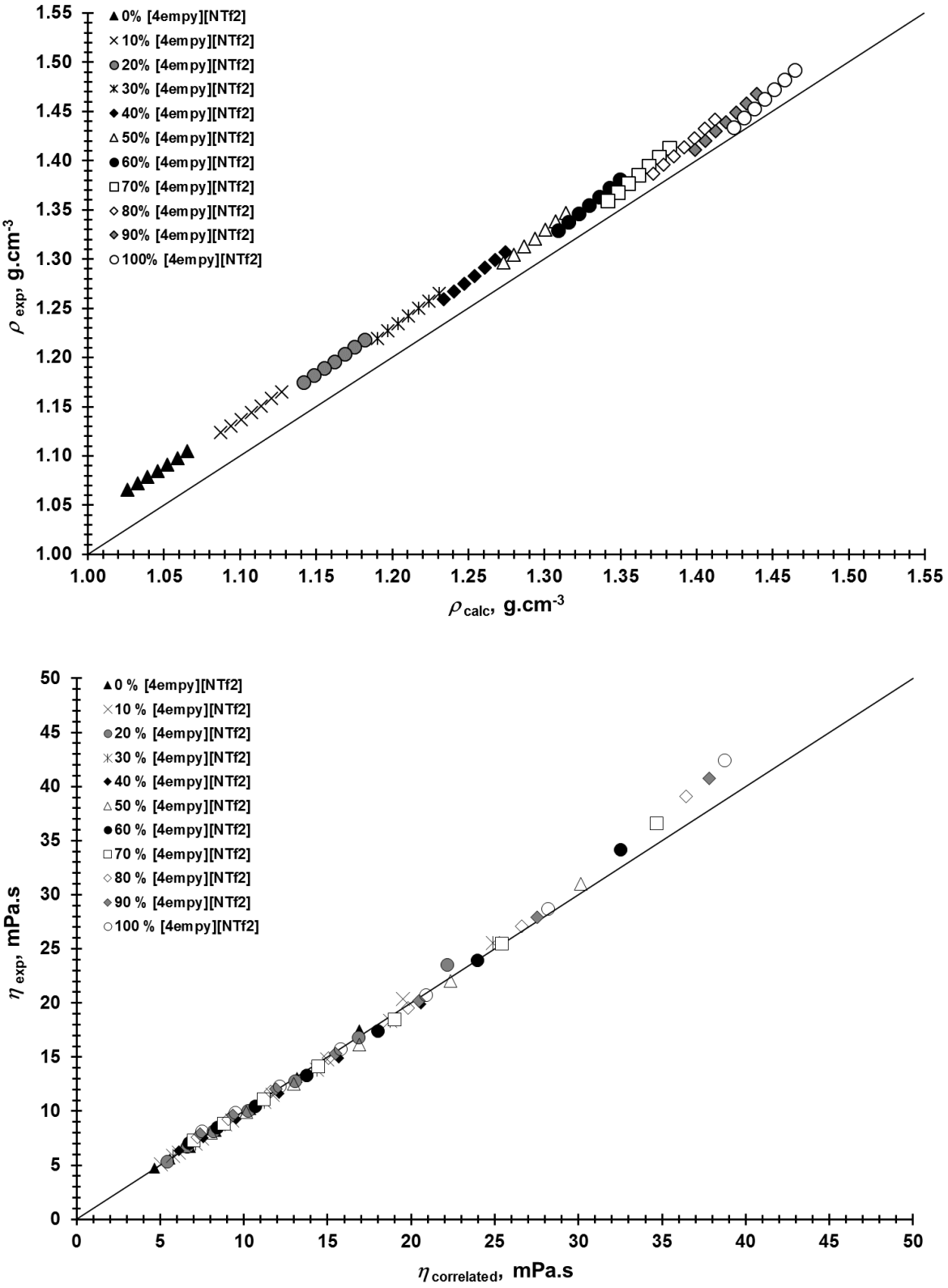

Fig. 10. Densities and dynamic viscosities of the {[4empy][NTf_2] + [emim][DCA]} binary IL-IL mixture at temperatures between 293.2 K and 353.2 K as a function of molar composition. Experimental properties were taken from [10], calculated densities were obtained from COSMO-based methodology, whereas correlated viscosities were obtained using an Arrenius-type equation and the experimental data for the pure ILs taken from [10].

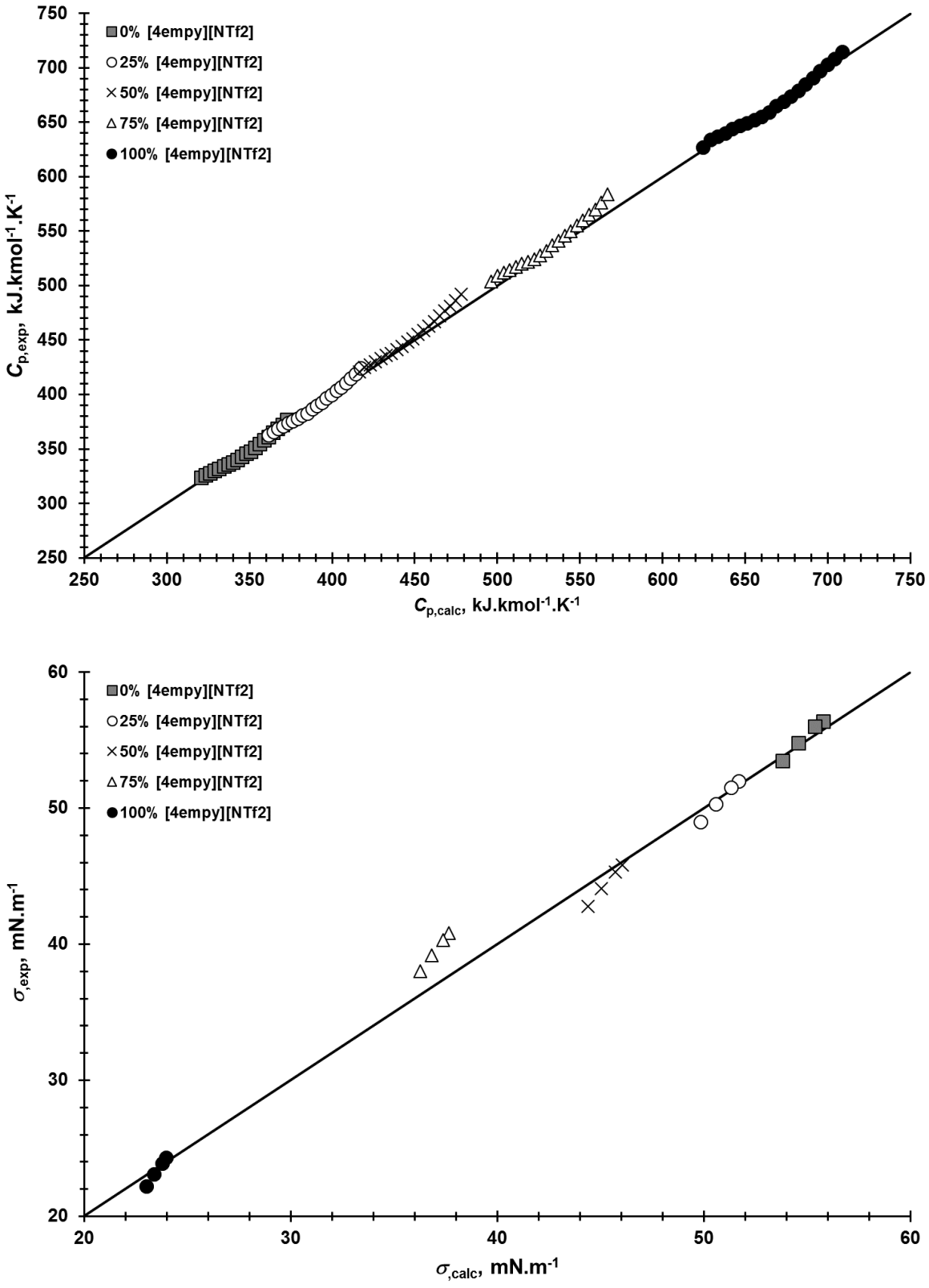

Fig. 11. Specific heats and surface tensions of the {[4empy][NTf_2] + [emim][DCA]} binary IL-IL mixture at temperatures between 293.2 K and 353.2 K as a function of mass composition. Experimental properties were taken from [43] and calculated properties were obtained from COSMO-based methodology.

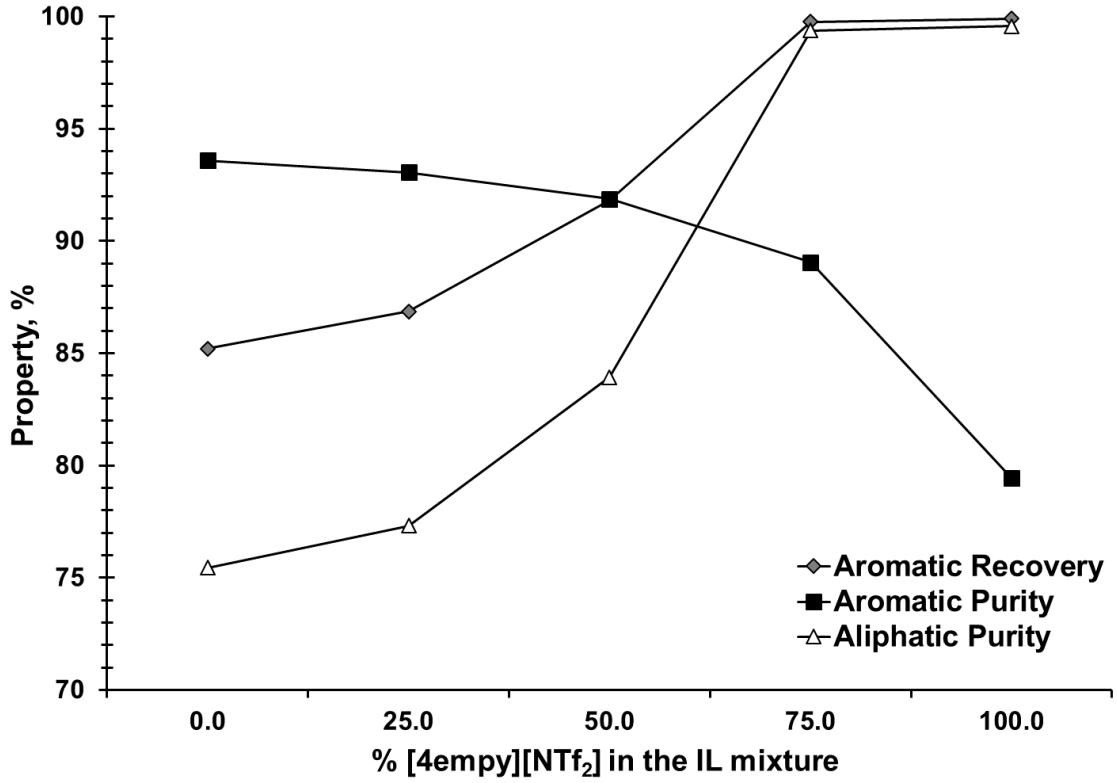

Fig. 12. Aromatic recoveries, aromatic purities in the product, and aliphatic purities in the raffinate (wt.%) using the Configuration 1 as a function of [4empy][NTf_2] mass fraction in the {[4empy][NTf_2] + [emim][DCA]} binary IL-IL mixture.

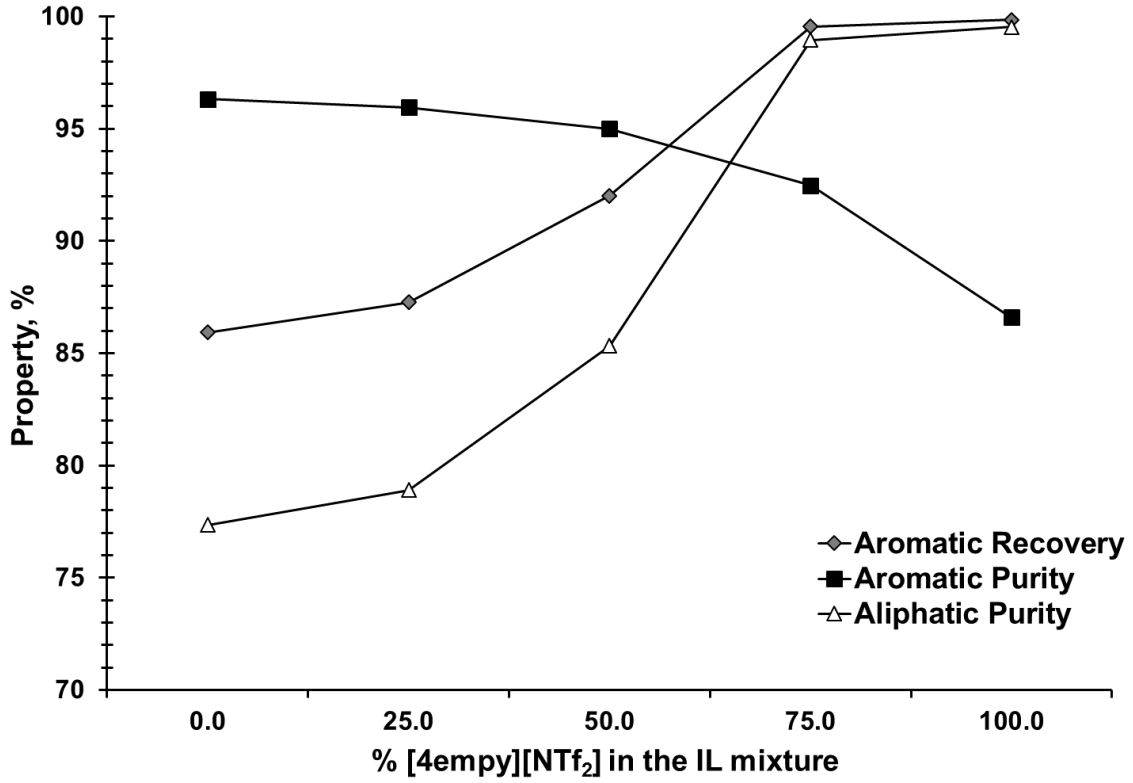

Fig. 13. Aromatic recoveries, aromatic purities in the product, and aliphatic purities in the raffinate (wt.%) using the Configuration 2 as a function of [4empy][NTf_2] mass fraction in the {[4empy][NTf_2] + [emim][DCA]} binary IL-IL mixture.

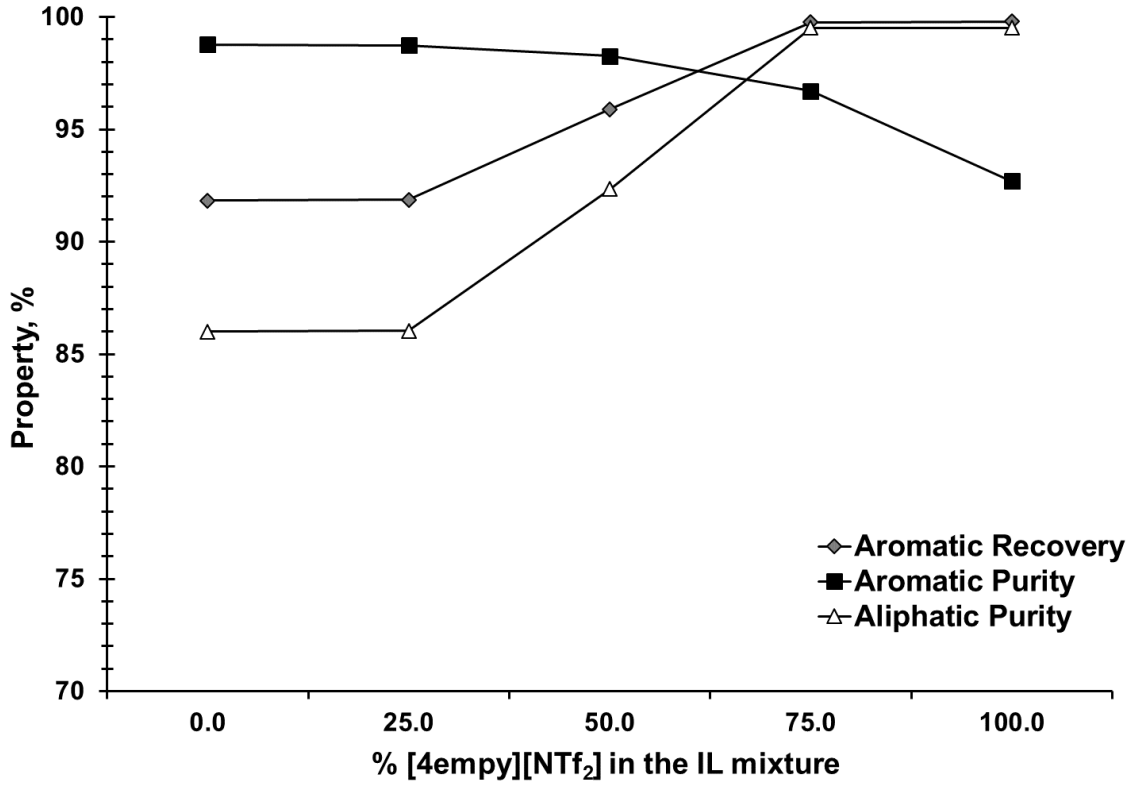

Fig. 14. Aromatic recoveries, aromatic purities in the product, and aliphatic purities in the raffinate (wt.%) using the Configuration 3 as a function of [4empy][NTf_2] mass fraction in the {[4empy][NTf_2] + [emim][DCA]} binary IL-IL mixture.

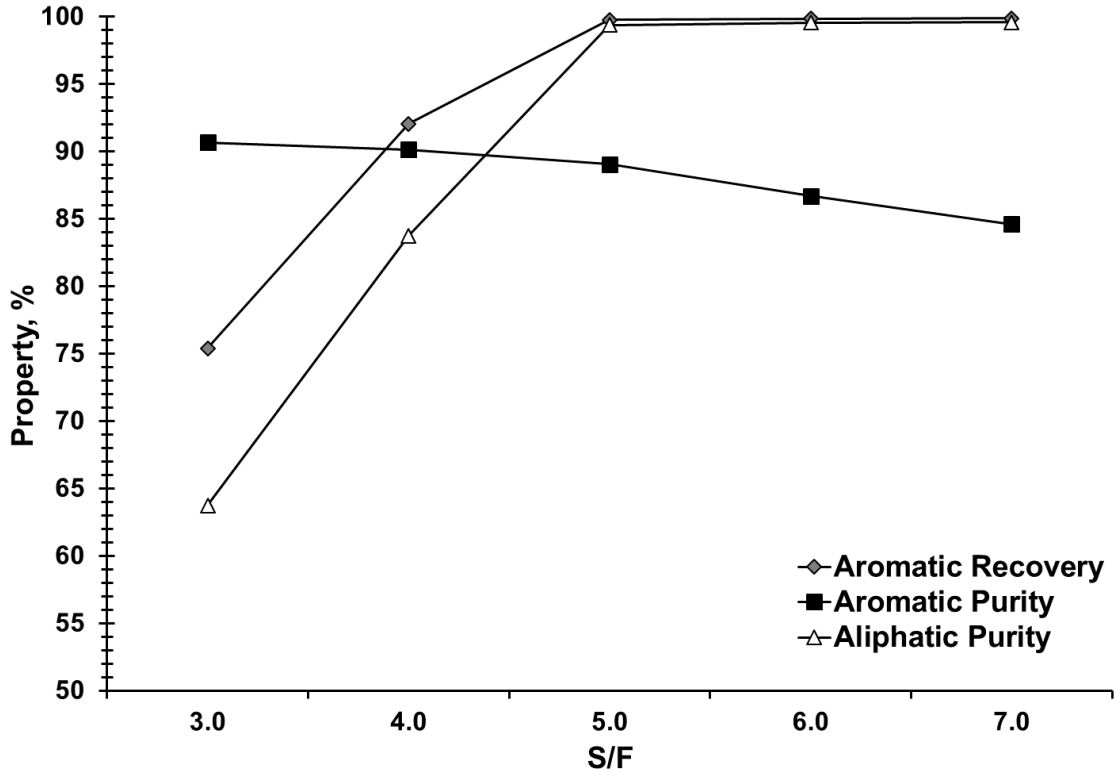

Fig. 15. Aromatic recoveries, aromatic purities in the product, and aliphatic purities in the raffinate (wt.%) using the Configuration 1 and the {[4empy][NTf_2] (75 %) + [emim][DCA] (25 %)} binary IL-IL mixture as solvent as a function of the solvent to feed ratio (S/F).

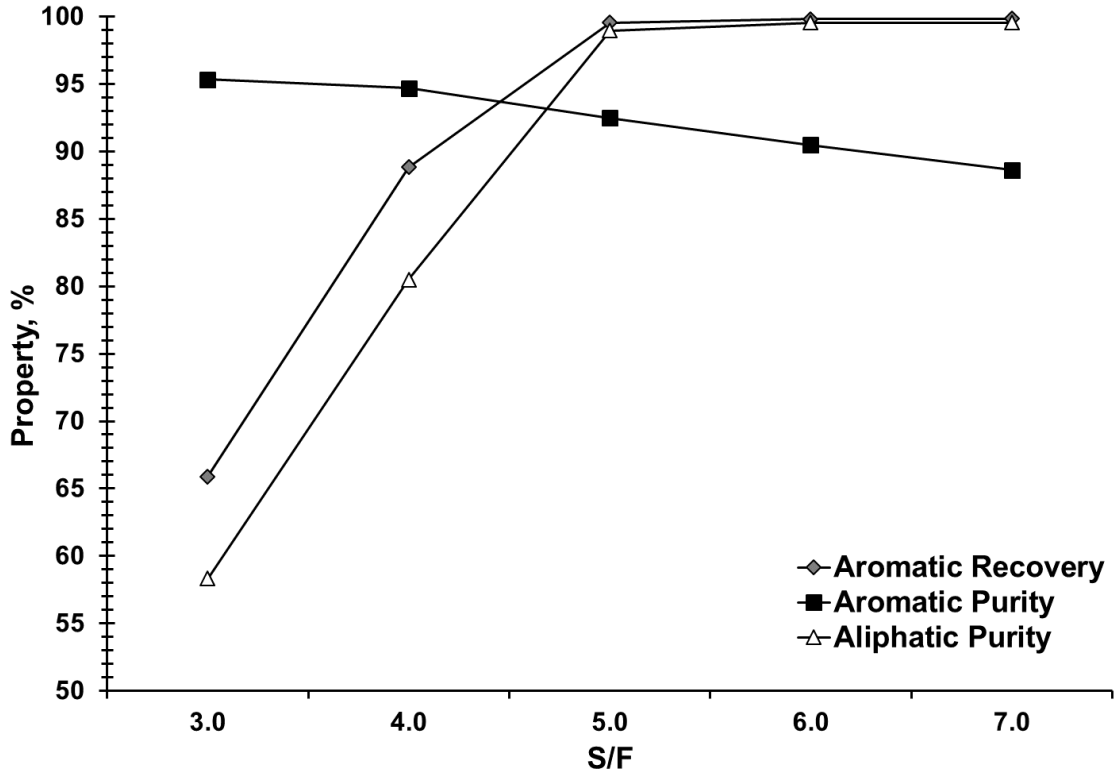

Fig. 16. Aromatic recoveries, aromatic purities in the product, and aliphatic purities in the raffinate (wt.%) using the Configuration 2 and the {[4empy][NTf_2] (75 %) + [emim][DCA] (25 %)} binary IL-IL mixture as solvent as a function of the solvent to feed ratio (S/F).

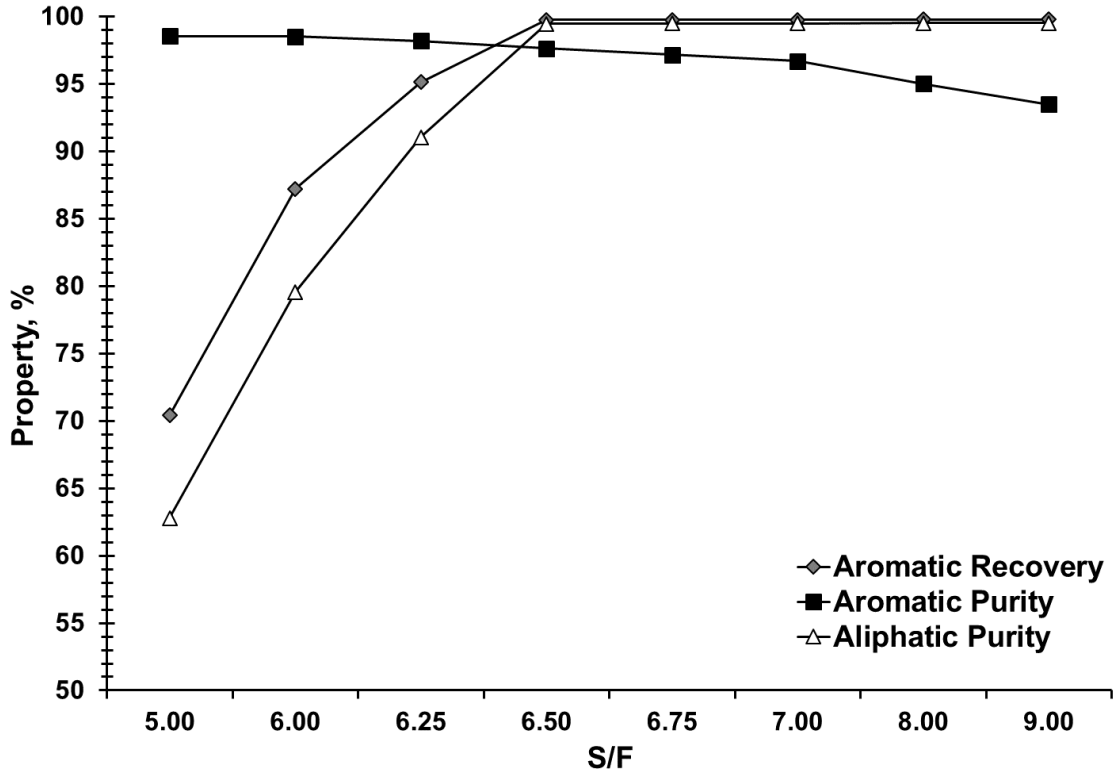

Fig. 17. Aromatic recoveries, aromatic purities in the product, and aliphatic purities in the raffinate (wt.%) using the Configuration 3 and the {[4empy][NTf_2] (75 %) + [emim][DCA] (25 %)} binary IL-IL mixture as solvent as a function of the solvent to feed ratio (S/F).

Table 1

Mass-based composition of the pyrolysis gasoline obtained by severe cracking

Hydrocarbon	wt.%
n-Hexane	11.3
n-Heptane	11.3
n-Octane	11.3
Benzene	33.8
Toluene	19.3
p-Xylene	13.0

Table 2

Correlation coefficients (R^2) and mean deviation of composition (Δx) in the fitting of experimental compositions against predicted compositions using COSMO-based/ASPEN methodology for the liquid-liquid equilibria of binary or pseudobinary systems

Ternary or Pseudoternary System	R^2	Δx
n-heptane + toluene + [emim][DCA]	0.998	0.011
n-heptane + toluene + [4empy][NTf_2]	0.984	0.039
n-hexane + toluene + {[4empy][NTf_2] (0.3) + [emim][DCA] (0.7)}	0.981	0.034
n-heptane + toluene + {[4empy][NTf_2] (0.3) + [emim][DCA] (0.7)}	0.986	0.026
n-octane + toluene + {[4empy][NTf_2] (0.3) + [emim][DCA] (0.7)}	0.992	0.019

Table 3

Correlation coefficients (R^2) and mean deviation of pressure (ΔP) in the fitting of experimental pressures against predicted pressures using COSMO-based/ASPEN methodology for the vapor-liquid equilibria of binary or pseudobinary systems

Binary or Pseudobinary System	R^2	ΔP / kPa
n-heptane + [emim][DCA]	0.932	3.6
toluene + [emim][DCA]	0.993	1.5
n-heptane + [4empy][NTf_2]	0.887	4.9
toluene + [4empy][NTf_2]	0.987	2.5
n-hexane + {[4empy][NTf_2] (0.3) + [emim][DCA] (0.7)}	0.915	9.4
n-heptane + {[4empy][NTf_2] (0.3) + [emim][DCA] (0.7)}	0.912	4.2
n-octane + {[4empy][NTf_2] (0.3) + [emim][DCA] (0.7)}	0.955	1.4
benzene + {[4empy][NTf_2] (0.3) + [emim][DCA] (0.7)}	0.976	6.5
toluene + {[4empy][NTf_2] (0.3) + [emim][DCA] (0.7)}	0.983	1.4
p-xylene + {[4empy][NTf_2] (0.3) + [emim][DCA] (0.7)}	0.982	0.9

Table 4

Correlation coefficients (R^2) and mean deviation of each physical property ($\Delta Prop$) in the fitting of experimental properties against estimated properties using COSMO-based/ASPEN approach for the densities, viscosities, specific heats, and surface tensions of the {[4empy][NTf_2] + [emim][DCA]} binary IL-IL mixture

Physical Property	R^2	$\Delta Prop$
Density	0.998	0.03 $g \cdot cm^{-3}$
Dynamic Viscosity	0.995	0.44 mPa·s
Specific heat	0.998	3.72 $kJ \cdot kmol^{-1} \cdot K^{-1}$
Surface Tension	0.987	0.91 $mN \cdot m^{-1}$

Table 5

Heat, cooling, and total energy needs of the three configurations as a function of composition in the {[4empy][NTf_2] + [emim][DCA]} IL mixture

Configuration 1 with a S/F mass ratio of 5.0			
% [4empy][NTf_2] in the mixture	Heat Needs	Cooling Needs	Total Energy Needs
	MW		
0.0	-112.7	93.1	205.8
25.0	-111.4	91.4	202.8
50.0	-112.2	91.0	203.2
75.0	-115.5	92.4	207.9
100.0	-119.1	93.8	212.8
Configuration 2 with a S/F mass ratio of 5.0			
% [4empy][NTf_2] in the mixture	Heat Needs	Cooling Needs	Total Energy Needs
	MW		
0.0	-110.3	89.6	199.9
25.0	-109.0	87.6	196.6
50.0	-109.6	86.9	196.5
75.0	-112.2	87.5	199.7
100.0	-116.9	86.8	203.7
Configuration 3 with a S/F mass ratio of 7.0			
% [4empy][NTf_2] in the mixture	Heat Needs	Cooling Needs	Total Energy Needs
	MW		
0	-148.7	115.6	264.3
25	-147.8	112.3	260.1
50	-147.8	110.2	257.9
75	-148.5	108.2	256.7
100	-154.2	105.6	259.8

Table 6

Aromatic recovery, aromatic purities in the product stream, aliphatic purities in the raffinate stream, and total energy needs using the Configurations 1, 2, and 3 at the optimal value of solvent to feed (S/F) ratio in mass

Configuration	S/F	Aromatic Recovery	Aromatic Purity	Aliphatic Purity	Total Energy Needs
	mass/mass	%	%	%	MW
1	5.0	99.8	89.1	99.4	207.9
2	5.0	99.5	92.5	99.0	199.7
3	6.5	99.8	97.7	99.5	250.1